Fiber-Optic Chemical Sensors and Biosensors (2008-2012)

ARTICLE *in* ANALYTICAL CHEMISTRY · NOVEMBER 2012

Impact Factor: 5.64 · DOI: 10.1021/ac303159b · Source: PubMed

2 AUTHORS, INCLUDING:

Xu-dong Wang
Fudan University
30 PUBLICATIONS **932** CITATIONS

SEE PROFILE

analytical chemistry

Review

pubs.acs.org/ac

Fiber-Optic Chemical Sensors and Biosensors (2008−2012)

Xu-Dong Wang* and Otto S. Wolfbeis*

Institute of Analytical Chemistry, Chemo- and Biosensors, University of Regensburg, D-93040 Regensburg, Germany

CONTENTS

Fiber-optics enable direct optical spectroscopy (from the infared to the ultraviolet; in absorption, emission and plasmonic resonance) to be performed at inaccessible sites, over large distances, in strong magnetic fields, and in harsh environment. If equipped with chemically responsive coatings, they also enable species to be sensed that are not directly amenable to optical spectroscopy. This review covers respective work published in the time period from January 2008 to September 2012 and is written in continuation of previous reviews.[1] Data were electronically searched in SciFinder and MedLine. In addition, the authors collected references from (sensor) journals over the past five years.

Given the number of articles published on fiber-optic chemical sensors and biosensors (FOCS), a stringent selection had to be made. Priority has been given to FOCS of defined chemical, environmental, or biochemical significance, to new schemes and new materials. This review does not include (a) FOCS that obviously have been rediscovered; (b) FOCS for monitoring purely technical processes such as injection molding, extrusion, or oil drilling, even though these represent important applications of optical fiber technology; and (c) sensors for temperature and other physical parameters. Regrettably, the assignment of some articles to specific sections sometimes is somewhat arbitrary, because some articles excel in terms of both new materials, advanced spectroscopic schemes, or analytical performance and selectivity.

Unfortunately, the term "sensor" has lost its clear definition over the past 10 years, and numerous articles are now published (mainly by organic chemists) where plain molecules ("molecular probes", "indicators") are referred to as "sensors". However, the definition[2] of chemical sensors (not only optical) is fairly unambiguous: "Chemical sensors are miniaturized analytical devices that can deliver real-time and online information on the presence of specific compounds or ions in complex samples". The most attractive but challenging feature of sensors is to yield online information and to work in complex, often flowing samples. Some of the so-called "sensors" published recently have turned out to be conventional cuvette tests without any (online) sensing capability. Publication only seems to be justified by using the term "sensor" in the title, one example being a "sensor" for CO_2 that is inferior to any other sensor for CO_2 and even any cuvette test for this gas.[3] It works in acetonitrile solution (who on Earth wants to sense CO_2 in acetonitrile?), requires the presence of a constant level of fluoride, effects occur deep in the UV (where almost any natural sample displays strong intrinsic absorption and fluorescence), and does not enable CO_2 to be continuously sensed over time. How shall such a "sensor" ever be used to monitor CO_2 in blood or seawater?

Optical analysis of a solution by adding an appropriate indicator probe in a cuvette sometimes also is referred to as "sensing" (to the surprise of the sensor community). One further comment is related to the lack of even a minimum of data on the selectivity and limits of detection of probes and sensors. Not any interaction between two species (particles included) is worth a paper on a new "sensing" scheme. Acetone, for example, is not a good "sensor" for solvent polarity, even though its carbonyl band in the IR depends on solvent polarity. A final criticism is related to the fact that certain authors do not seem to be aware of the state of art in sensor technology and do not cite (or read?) articles in sensor journals and analytical journals.

Fiber-optics serve analytical sciences in several ways. Plain fiber-optics enable optical spectroscopy to be performed at sites inaccessible to conventional spectroscopy, over large distances,

Special Issue: Fundamental and Applied Reviews in Analytical Chemistry 2013

Published: November 9, 2012

   dx.doi.org/10.1021/ac303159b | *Anal. Chem.* 2013, 85, 487−508

or even on several spots along an optical fiber. Second, in being optical waveguides, fiber-optics enable less-common methods of interrogation, in particular evanescent wave spectroscopy and spatially resolved lifetime spectroscopy. Fibers are available now with transmissions over a wide spectral range. There is a need for long-wave sensing where background signals (from fibers and samples) are weaker and (laser) light sources are less expensive.

Major fields of applications of FOCS are in sensing gases and vapors, in medical and chemical analysis, molecular biotechnology, marine and environmental analysis, industrial production monitoring and bioprocess control, and the automotive industry. [*Note:* In this article, sensing refers to a continuous process, while probing refers to single-shot testing. Both have their fields of applications. Admittedly, biosensors based on immunoaffinity or polynucleotide interactions are unlikely ever to work in a fully reversible way. Respective devices have been termed biosensors for decades now (mainly by the medical and diagnostic community), and this terminology is accepted here.]

FOCS are based on either direct or indirect (recognition-based) sensing schemes. In the first, the intrinsic optical properties of an analyte (such as its color or fluorescence) are measured. In the second, the color or fluorescence of an immobilized indicator probe, of a metal film or a (nano)material, or an optically detectable label is monitored. Another active area of research includes advanced methods of interrogation such as time-resolved or spatially resolved spectroscopy, evanescent wave and laser-assisted spectroscopy, (localized) surface plasmon resonance, leaky mode spectroscopy, and multidimensional data acquisition. Fiber bundles also have been employed for the purposes of imaging, biosensor arrays (along with encoding), or use as arrays of nonspecific sensors whose individual signals may be processed via artificial neural networks. The use of advanced nanomaterials is growing rapidly and has led to impressive innovations.

BOOKS, REVIEWS, AND ARTICLES OF GENERAL INTEREST

The progress made in the field of FOCS has been reviewed from various points of view. General aspects of FOCS are treated in a book edited by Udd and Spillman.[4] It mainly covers sensors for physical parameters but also contains a chapter on fiber-optic biosensors, with sections on optical sensor technologies, sensor classes, transducer mechanisms, and configurations, and another chapter that covers distributed and multiplexed fiber-optic sensors, with a focus on distributed and multiplexed sensing, and specifically on interferometric multiplexing. These are also of interest in the context of chemical and biochemical sensing. Chemical sensors and biosensors based on fluorescence and phosphorescence have been categorized.[5] Biosensors have been subdivided into subgroups according to their mode of action: (a) plain fluorometric sensors, (b) direct and indirect indicator-mediated chemical sensors, (c) direct enzymatic biosensors, (d) indicator-mediated enzymatic biosensors, and (e) affinity biosensors. The discussion is accompanied by examples and further subdivisions for some sensor types.

Materials science aspects also have received substantial attention. In their review on nanomaterials in fiber-optic sensors in healthcare and industry applications, Sun et al.[6] show that materials such as metal nanoparticles and carbon nanotubes can dramatically improve the performance and functionality of optical fiber sensors for use in structural health and environmental monitoring, and in biomedical imaging. Another review[7] covers the progress made in the development of indicator-based materials for use in chemical sensing and imaging, especially for analytes such as oxygen, pH value, CO_2, ammonia, and glucose. Respective "sensor paints"[8] are placed on the surface of a sample such as skin or at the tip of an optical fiber. Pressure- and temperature-sensitive paints form another field of applications. Such "paints" respond to a (bio)chemical parameter with a change in their optical properties.

Tao and Guo[9] have reviewed spectroscopic techniques (mainly in the infrared) for fiber-optic gas detection, and Duffin et al.[10] described the state of the art in optical chemical sensor networks for gas detection and environmental monitoring. Such sensors often work in hostile environments, yet possess adequate sensitivity for most applications, and automatic recalibration of both zero-point and scale factor. Some are capable of yielding information on gas concentration and temperature simultaneously. Fiber-optic sensors for biological and chemical agent detection have been reviewed by Aernecke and Walt.[11] The authors discuss the general utilization of optical fibers as sensors, and present specific examples where (fiber) optic platforms have been applied to detect biological and chemical warfare agents. Multiple parameter (and multiwavelength) fluorescent chemical sensing and imaging has attracted much attention, because several species can be sensed simultaneously and at the same site by optical (fiber) sensors.[12] Such sensors are making use of probes whose signals can be differentiated by spectral and/or temporal resolution. Multiple sensors are of substantial interest for continuous monitoring of chemical parameters in complex samples such as blood, bioreactor fluids, in the chemical industry, aerodynamic research, and when monitoring seawater or food quality. The single chapters cover spectroscopic principles, materials (mainly indicator probes and polymers), and selected examples for dual and triple sensors (see Figure 1).

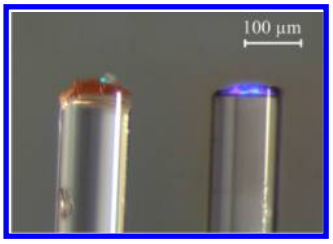

Figure 1. Photographic images of fiber-optic dual microsensors. The left-side sensor tip (for oxygen and temperature) displays both a green color (that results from the green LED light source) and a red fluorescence of the dual sensor. The right-hand sensor tip (pH/O_2) displays the blue color of the 470-nm LED, along with red and green luminescence that originates from the respective luminescent probes. (Reprinted with permission from ref 13. Copyright American Chemical Society, Washington, DC, 2007.)

Sanz-Medel et al.[14] have critically compared different ratiometric techniques for fiber-optic luminescence sensing. Measurement of luminescence intensity suffers from a series of analyte-independent fluctuations, which make them less appropriate for chemical sensing purposes. Lifetime is one attractive alternative, but ratiometric measurements are simpler, at least in principle. Two methods based on ratiometric techniques were compared. The first is a ratiometric method working in the frequency domain, and the other is a wavelength ratiometric method.

In order to better exploit incident light and, thus, enhance the brightness of luminescent sensors, a smart scheme was introduced to improve the emissive output of indicator dyes.[15] Emission is amplified by the addition of antenna dyes in high concentration, These absorb the excitation light and transfer it to an

dx.doi.org/10.1021/ac303159b | *Anal. Chem.* 2013, 85, 487−508

indicator dye. This harvesting of light enables sensor layers to be as thin as <500 nm. Possible applications of light harvesting to various reagent-mediated optical sensing schemes are given.

Fiber-optic biosensing is an "evergreen". Ligler and Taitt[16] have published the second edition of their book on optical biosensors. It contains numerous updates and sections on evanescent-wave fiber-optic biosensors, optrode type of biosensors (where the signals are generated by a sensing layer usually composed of biorecognition element and dyes, all attached to the end of the fiber), planar waveguide biosensors, biosensors based on SPR or surface-enhanced Raman spectra (SERS), and fluorescence-lifetime-based biosensors, among others. Recent advancements in bio-optrode technologies include the development of nanoscale bio-optrodes, enabling measurements inside single living cells, and the development of multianalyte and reagentless bio-optrodes. A review on optical biosensors in general also covers fiber-optic biosensors[17] and contains sections on (a) enzymatic biosensors, (b) immunosensors, (c) biosensors based on ligand−receptor interactions, (d) nucleic acid biosensors, (e) whole cell biosensors, and (f) new materials for use in optical biosensors.

Current trends in fiber-optic chemical and biological sensors were summarized by Orellana and Haigh,[18] with a focus on indicator mediated (rather than direct spectroscopic) sensors. Gas "optodes" (for oxygen, hydrogen, carbon dioxide, and ammonia), humidity sensors, monitors for pH, cations and anions, and sensors for organic compounds are treated in respective sections. Biosensors based on the use of enzymes, antibodies, nucleic acids, and entire micro-organisms illustrate the state of the art in this field. Selected examples are given for absorbance-based, luminescent, evanescent wave, Fabry−Perot, chemiluminescent, and SPR-based sensors and biosensors. The state of the art in technologies for fiber-optic sensing of humidity and moisture was also reviewed,[19] with an introduction into conventional detection methods, this followed by a review on both intrinsic and extrinsic fiber-optic sensor configurations. The state of the art in optical methods for sensing glucose (the in vivo sensor for glucose being the holy grail in biosensing) has been reviewed.[20] Following an introduction into the significance of (continuous) sensing of glucose and a brief look back, methods are discussed that are based on (a) monitoring the optical properties of intrinsically fluorescent or labeled enzymes, their coenzymes and cosubstrates; (b) the measurement of the products of enzymatic oxidation of glucose by glucose oxidase; (c) the use of synthetic boronic acids; (d) the use of Con A; and (e) the application of other glucose-binding proteins. The advantages and disadvantages of the methods are critically assessed.

Reviews that partially cover the field of fiber-optic sensors include those on optical chemical sensors in general,[2] and on luminescent chemical sensing, biosensing, and screening using UCLNPs,[21] which display the unique property of converting near-IR light (with wavelengths of typically 800−1000 nm) into visible luminescence. One typical application of such nanoparticles is to act as nanolamps whose emission intensity is modulated by chemical indicators placed in their vicinity (such as in sensor films).[22] This method may be applied to all systems for which a spectral match does exist between the emission of UCLNPs and the absorption of an indicator probe.

■ SENSORS FOR (DISSOLVED) GASES AND VAPORS

This section covers all room-temperature gaseous species including their solutions in liquids. One major research focus is on hydrogen and methane, because both are highly explosive when mixed with air. They may be sensed more safely with FOCSs than with electrical devices.

Hydrogen. Hydrogen is a clean and inexhaustible source of energy. It is considered a future fuel, because its oxidation does not produce atmospheric products that cause global warming. However, hydrogen gas leaks readily and is highly explosive above a critical concentration. Therefore, the development of sensors to detect hydrogen leakage is important wherever hydrogen is used. Potential applications are in hydrogen-powered cars, aircrafts, space vehicles, and in liquid hydrogen production and storage facilities. Thus, respective sensors are likely to become mass products. (Fiber)-optic sensors for hydrogen are based on optical signals and do not imply the risk of producing electrical sparks or discharges. In addition, FOCS for hydrogen have small size and can access sites that may be hardly accessible for electronic devices.

Molecular hydrogen does not possess an intrinsic absorption or emission that may be exploited in optical sensing. Therefore, it is detected indirectly by virtue of the fact that it strongly binds to films of metallic platinum (Pt) and palladium (Pd), whose dielectric properties are changed as a result. Several hydrogen sensors have been developed based on this principle, as summarized in previous reviews of this series. More recently, Monzón-Hernández et al. have described the response of fiber-optic hydrogen sensors, based on the use of Pd and gold (Au) nanolayers.[23] They coated heterocore optical fibers with 1.4-nm layers of Pd and 0.6-nm layers of Au by thermal evaporation. The presence of hydrogen produces a decrease in the palladium refractive index (RI), which causes a change in the attenuation of the optical fiber evanescent wave. The sensors have fast response (4.5 s) and short recovery times (13 s). Silva et al.[24] have reviewed the state of the art of Pd-based FOCS for hydrogen. Three sensing schemes (interferometry, measurement of intensity, and fiber grating techniques) are discussed, and the characteristics and sensing performances of these sensors were reviewed.

A transducer layer with a multilayer stack (layers of silver, silica, and Pd that acts as active components) was deposited on a multimode fiber without an optical cladding, and the spectral modulation of the light transmitted by the fiber was used for detecting hydrogen.[25,26] Interestingly, the sensor is sensitive to the transverse magnetically polarized light only, while the transverse electrically polarized light can act as a reference signal. The sensing performance can be tuned by varying the thickness of the multilayer. The silica thickness tunes the resonant wavelength, whereas the silver and Pd thickness determines the sensitivity of the sensor. A FOCS for hydrogen based on SPR was built by coating silver, silicon, and Pd layers on an unclad core of a fiber.[27] The presence of hydrogen in the air around the Pd coating changes the dielectricity of the Pd layer and results in a shift in the SPR wavelength that can be utilized to sense hydrogen. The wavelength shift initially increases with time and then saturates. The presence of a silicon layer enhances the shift in resonance wavelength and can increase precision.

Tungsten trioxide (WO_3) supported with Pt metal has often been employed to sense hydrogen.[28] This material was chosen because the reduction of WO_3 (which itself is not reactive to hydrogen) readily proceeds in the presence of noble-metal catalysts such as Pt or Pd. Hydrogen molecules on the surface of metal catalysts dissociate to form adsorbed hydrogen atoms (H_{ad}), even at room temperature. They react with WO_3 through a spillover process and reduce it to tungsten bronze. The reaction is accompanied by a distinct color change from a grayish semitransparent color to dark blue. Strong absorption occurs due

dx.doi.org/10.1021/ac303159b | Anal. Chem. 2013, 85, 487−508

to this chromogenic reaction. The RI of the film also is altered and results in transmission losses of the fiber-optic system. Evanescent field interaction with the Pd/WO_3 cladding is the preferred method for readout. If exposed to 1 vol % of hydrogen in air or nitrogen gas, the changes in optical power propagating through the fiber are ~30% and ~50%, respectively. However, the relative humidity (RH) interferes and lowers the response time. The reaction is only partially reversible upon adding an oxidizing agent such as oxygen to generate nonreduced WO_3 again. The same group[29] has optimized the thickness of the WO_3 layer to decrease propagation losses.

The same Pt/WO_3 coating was used[30] for sensing hydrogen in a very different way. When WO_3 reacts with hydrogen through catalysis by Pt, thermal energy is released, which causes a local increase in temperature. There is a relationship between the center wavelengths of a fiber Bragg grating (FBG) and the rise in temperature. This can be expressed by the equation

$$\Delta\lambda_B = (\alpha + \xi)\Delta T\lambda_B$$

where α is the expansion coefficient and ξ is the thermo-optic coefficient. The center wavelength shift of the FBG can be used to calculate the concentration of hydrogen. The response time is short (~10 s), and the response to low hydrogen levels (below 4%) is linear. The sensor works at levels of up to 50% of hydrogen but its response is nonlinear and the material requires >2 min until full recovery. Since the method is based on the measurement of ΔT, precise control of T is mandatory, which may limit practical applications in certain situations and in distributed sensing. A similar scheme for hydrogen sensing was reported using acoustically induced long-period grating (LPG).[31]

Okazaki et al.[32] constructed a FOCS for hydrogen comprised of a bismuth-based fiber core and a sol−gel-derived platinum-supported WO_3 thin film (Pt/WO_3) as a sensing clad. The RI of this type of fiber core is higher than that of the Pt/WO_3 cladding so that the absorption of evanescent-wave leaking from the fiber core into the clad region causes a propagation loss. This was used as the optical information for sensing hydrogen. The light power propagating through a 5-cm fiber exposed to 10% hydrogen gas decreased by ~10%. However, this sensor faces the same material problems as those discussed above.

Rather than using Pt/WO_3, one may also use plain palladium metal, because it is capable of reversibly binding hydrogen. A long-period fiber grating (LPFG) was coated[33] with a nanostructured palladium layer in order to sense hydrogen at temperatures between 30 °C and 200 °C. The response is the result of a change of the RI of the palladium layer upon exposure to hydrogen that causes the resonance wavelength of the LPFG to shift. The palladium layer was prepared by sputtering and mainly consists of nanograins 30−40 nm long. The resonance wavelength of the LPFGs coated with this material decreases as the hydrogen concentration increases from 0% to 16%. The sensor has a short response time (<70 s) and maintains its functionality for several cycles of detection and recovery, but the recovery times become increasingly long.

A proton-conducting perovskite oxide thin film was integrated[34] into a LPFG device for measurement of hydrogen in fossile- and biomass-derived synthetic gas at temperatures as high as 500 °C. A thin film of $Sr(Ce_{0.8}Zr_{0.1})Y_{0.1}O_{2.95}$ nanocrystals (referred to as SCZY) was coated onto the 125-μm-diameter LPFG, and the LPFG resonant wavelength was found to be a function of the RI of the overcoat. At high temperature, the ionic and electronic defects in the SCZY depend on the local partial pressure of hydrogen and, thus, shift the resonant wavelength of the LPFG. This sensor also has a good thermal stability for more than 100 h of operation, is reversible, sensitive, and stable over a wide range of hydrogen concentration even at high temperature. The selectivity of the sensor over gases such as CO, CO_2, CH_4, water vapor and H_2S is rather good. All these features make this sensor well-suited for in situ sensing of hydrogen at high temperatures.

Hydrogen usually is stored at high pressure and/or in liquid form. Therefore, instrumentation for continuous sensing of liquid (or highly compressed) hydrogen is highly desirable. A recent approach[35] to detect hydrogen in high-pressure gas mixtures is based on a microstructured twin hole FBG where the variation of RI of silica upon exposure to hydrogen gas results in a shift of the Bragg resonance. The microstructured fiber design allows hydrogen to rapidly diffuse into and out of the fiber core, and this results in fast response. Liquid-phase hydrogen also was shown[36] to be detectable by refractometry via a small hemispherical sensor element of fused silica linked to two multimode optical fibers. Liquid hydrogen and gaseous hydrogen have rather similar refractive indices so that optical fibers with a small angular aperture must be used. If properly positioned, a substantial loss of non-liquid-dependent light is observed. Such sensors are intrinsically safer than electrochemical sensors, potentially less expensive, and can be used as a point device or in multipoint arrays.

Hydrocarbons. Hydrocarbons usually are detected by virtue of their weak absorption (that is caused by methyl and methylene groups) in the infrared (IR) between 2900 cm^{-1} and 3000 cm^{-1}. Sensors for methane are needed in the gas and oil industry in general, as detectors in homes heated with gas, in coal mines, and in studies related to the greenhouse effect of methane gas. Methane, the most important analyte, has two vibrational absorption bands, viz, the $\nu_2 + 2\nu_3$ combination band centered at 1.33 μm, and the $2\nu_3$ overtone band peaking at 1.67 μm. The $\nu_2 + 2\nu_3$ band of methane is weak and interfered by water vapor. The band located at 1.67 μm is ~1 order of magnitude stronger than the $\nu_2 + 2\nu_3$ band and therefore widely used for purposes of direct spectroscopic sensing. Wang et al.[37] developed a technique for methane detection using wavelength scanning of a distributed-feedback laser. The absorption band at 1.67 μm serves as the analytical wavelength for sensing methane in the 0%−30% concentration range. Such (reagentless) direct sensors have excellent long-term stabilities, in the given case at least 4 months, and a precision of ±0.05%. This sensor is intended for use in coal mines.

IR absorption bands have relatively low molar absorbances (compared to those of electronic transitions). In order to achieve detectable absorbances, multiple absorptions (e.g., via evanescent waves) or extended optical pathways must be generated. Wu et al.[38,39] have fabricated a sensor for methane based on a sampled fiber grating and a differential absorption technique, where equally spaced multiabsorption lines of methane in the NIR were detected simultaneously. A comb-shaped filter enables three absorption lines of methane at ~1.67 μm to be measured at the same time. A reference grating provides a referenced signal and allows ratiometric measurements so to eliminate the adverse effect of unstable light sources and photodetectors. Another option to increase the limits of detection is to pass the sample gas through a hollow fiber.[40,41] This warrants long interaction lengths, low limits of detection (10 ppm; v/v), and is technically simple. The hollow fiber also may be coiled, and this results in more-compact devices. However, this also implies long filling and pass times (10 min). Another fiber loop method for sensing methane employs a 50-mm gap.[42] A pulse of light with a

dx.doi.org/10.1021/ac303159b | Anal. Chem. 2013, 85, 487−508

wavelength of 1665 nm is coupled into the loop and is reflected four times in the gas chamber (in the sense of a White cell). Such flow-cell direct spectroscopic sensors are simple and reliable, and the error in the given case is <3%. However, ambient light and other gases may interfere.

Acetylenes lack methylene groups and thus cannot be sensed via the respective IR absorptions. Multipoint chemical sensing of acetylene was demonstrated using frequency-shifted interferometry.[43] Frequency-shifted interferometry was applied to interrogate multiple gas sensors along a single fiber. This method uses a tunable continuous-wave laser and a slow detector, and allows spectral overlap of sensors. It can be used to quantify the concentrations of single or different gas species at multiple locations. A three-sensor system was used to demonstrate this capability, achieving a minimal detectable acetylene concentration of 230 ppm with a 3-cm gas cell, or equivalently, 6.9 ppm. The design considerations in the implementation and the system parameters are also discussed. Many conventional hydrocarbons can be directly sensed in the IR with a SPR-based fiber-optic sensor covered with a conducting metal oxide film.[44] A theoretical analysis revealed that such a sensing probe is more sensitive by ~60% than a gold-coated fiber-optic sensor. The physical reasons behind sensitivity enhancement are provided. Advantageous features of the use of indium tin oxide over silver and gold are addressed.

It is well-known that the concentration of propane and other hydrocarbons can be determined via IR attenuation of the 2940 cm^{-1} absorption band that is due to fundamental CH-stretch vibrations of these species. A fiber-optic sensor was described for continuous monitoring the local fuel concentration at the ignition position in spark-ignited engines which represents a rather harsh environment.[45] A tungsten halide lamp served as an IR light source. The sensor was calibrated using various hydrocarbon test gases at pressures up to 1800 kPa and at temperatures between 298 and 473 K.

Oxygen. Oxygen sensing remains another area where FOCS are quite successful. This is also corroborated by the number of companies that are manufacturing optical sensors for oxygen, examples being Presens (probably the largest; www.presens.de/); PyroScience (www.pyro-science.com/); Centec (www.centec.de/); Ocean Optics, Inc. (www.oceanoptics.com/); Oxysens, Inc. (www.oxysense.com/); Finesse, Inc. (www.finesse.com/); and Hach-Lange GmbH (www.hach-lange.de), to mention the larger ones. In the medical field, OptiMedical Systems, Inc. (www.optimedical.com/) probably is the largest. Oxygen is optically sensed almost exclusively by virtue of the quenching effect that it exerts on certain fluorophores, mainly complexes of Ru(II), Ir(II), Pt(II), and Pd(II). Respective sensors have distinct features such as high spatial resolution (<50 μm), high temporal resolution (t_{90} < 1 s), and an analytical range from 1 ppb up to 22.5 ppm of (water)-dissolved oxygen. Such sensors also have the option of using probes whose luminescence is less strongly quenched by oxygen and therefore can be used to sense high concentrations (or pressures). Additional features include the lack of consumption of oxygen, an optical signal that is independent of flow velocity, and the option of measuring oxygen both in liquids and in the gas phase. Optical oxygen sensors have found extensive applications in recent years, also because they can be operated in highly explosive areas and because they are not interfered by electromagnetic fields such as in hyperthermal cancer treatment. Wang et al.[46] have summarized recent developments in such sensors, with sections on new oxygen probes, new supporting materials, novel methods for optical interrogation, and respective assays.

Durable fiber-optic oxygen sensors were developed for harsh underground environments.[47] The sensor materials consisted of a silicone resin containing a luminescent Ru(II) diimine complex that is quenched by oxygen. The sensor film is very stable, even in hot water (80 °C), and its sensitivity remains stable over time if the sensor film is coated with a thin layer of silicone. FOCSs for oxygen for use in aircraft fuel tanks were critically assessed.[48] Various intensity-based approaches were contrasted with frequency-domain (lifetime) techniques, and a compact analytical system was suggested that uses the frequency heterodyning cross-correlation technique. Fiber-optic oxygen sensors also allow for long-term corrosion monitoring of radioactive-waste repositories.[49] A ruthenium complex with a dodecyl sulfate counterion was utilized as the oxygen-sensitive probe placed in a silicone resin. Degradation tests were conducted in air at temperatures between 150 °C and 250 °C and showed the sensor membranes to possess remarkable stability. A very similar sensor material was applied in a FOCS to study corrosion.[50] The sensor can detect as little as 0.9 Torr of oxygen in the gas phase, and 0.01 mg/L of oxygen in water solution. A robust device based on a similar sensor chemistry also was described for small-scale oxygen measurement in riverine sediments.[51]

Fiber sensors for oxygen are very well-suited to study the uptake of oxygen by HEPG2 liver cells encapsulated in alginate matrices.[52] The cells where grown (a) on cover glass slides, and (b) encapsulated within alginate-based hydrogel matrixes. It was concluded that the rate of oxygen uptake can be used as an indicative parameter to assess the metabolic activity of cells. Similarly, the respiratory activity of isolated mitochondria was investigated with a sensor for oxygen.[53] The study revealed that the respiratory activity of isolated mitochondria is functional for 3 h but ends at a critical limit of 20% air saturation. Bacterial growth also was monitored with an optical sensor for simultaneous measurement of dissolved oxygen and pH.[54] The sensor was used to monitor the growth of *Pseudomonas putida* cultures. The method is said to be well-suited for parallelized, miniaturized bioprocessing and for cell-based high-throughput screening applications. Bagshaw et al.[55] have applied fiber-optic oxygen sensors to study an extreme glacial environment. They compared their performance in icy ecosystems and under standard laboratory temperatures. The results showed the fiber-optic sensors to be reliable, precise, rapid, and practically free from signal drift. However, the survival of freeze−thaw cycles was problematic unless the sensor film was mechanically fixed on the fiber and protected by a stainless steel sheath.

Fluorinated polymers are the material of choice to host quenchable oxygen probes because of their high permeability for oxygen. Fluorinated xerogel films containing ruthenium(II) tris(2,2′-bipyridine) were employed[56,57] in fiber-optic sensors for dissolved oxygen. The luminescence of the probe in the sensing film is strongly quenched by oxygen. The sensor has a response time of 4 s, a limit of detection of 0.04 ppm of oxygen in water, and good long-term stability (10 months). The Stern−Volmer plot is linear so that two-point calibration is possible. The same group[58] prepared other gas-permeable fluorinated materials with even better performance. However, in both cases, the water-soluble tris(2,2′-bipyridine) ruthenium(II) in these fluorinated materials many face leakage problems while applying for dissolved oxygen sensing. If fiber-optic oxygen sensors are to be used in respiratory testing (such as in intensive care units (ICUs)), a very fast time (<0.1 s) is obligatory. A cylindrical-core fiber-optic sensor was developed,[59,60] where the oxygen-sensitive probe Pt-octaethylporphyrin was immobilized in poly(ethyl methacrylate)

dx.doi.org/10.1021/ac303159b | Anal. Chem. 2013, 85, 487−508

film and coated on silica optical fiber with a cylindrical core. The response time of this sensor is <50 ms, but the choice of materials is not perfect in that PtOEP is photolabile and polymers with better permeability are known.

Fast oxygen sensors are also needed for oceanography, which is a powerful tool for studying oxygen flow above the sea bed and in eddy. In this particular application, FOCS for oxygen have the advantage (over microelectrodes) of being insensitive to flow, less susceptible to signal drift, more durable under typical field conditions, and less expensive. Chipman et al.[61] developed a fast sensor (shown in Figure 2) to measure oxygen exchange across the sediment/water interface. It has a response fast

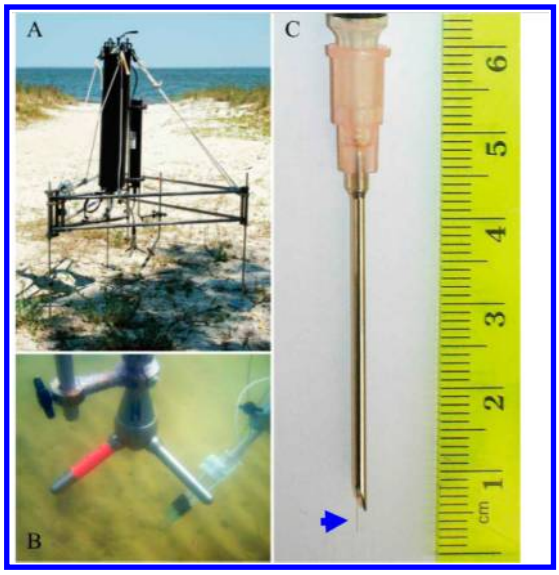

Figure 2. (A) Eddy correlation instrument with a fiber-optic sensor for oxygen. (B) Sensor head and two optodes. (C) Optical fiber sensor housed in a 4-cm syringe. The dark spot at the end of the glass fiber protruding from the needle (see the blue arrow) is the sensing dye. The dark line parallel to fiber is the shadow of the fiber. (From ref 61, Copyright 2012, Association for the Sciences of Limnology and Oceanography, Inc.)

enough (~160 ms) to capture the oxygen fluctuations that are relevant for the flux calculations. A similar sensor configuration was applied in an investigation of oxygen gradients within biofilms.[62]

Remote sensing was demonstrated[63] with a fiber-optic sensor for both oxygen or pH with magnetic control (Figure 3). Stainless steel spheres were coated with optical chemical sensors. Such spheres can either be reversibly attached to the tip of an optical fiber (dip-probe) or trapped inside a vessel for read-out through the side wall. Moving the magnetic separator at the exterior enables measurements at varying positions with a single sensor. The sensor can be rapidly replaced in a contactless mode. The sensor was successfully used for sensing oxygen or pH in stirred liquids, rotating flasks, and 24-well microplates. These properties resulted in strong but reversible fixation, magnetic remote controllability, short response times, high signal intensities, and simplified handling.

FOCS, unlike electrodes, have the unique capability of multiple sensing. Oxygen is often measured along with other parameters such as pH value or temperature. Simultaneous sensing of pH, oxygen, and temperature was accomplished with multicolor fluorescent and permeation-selective microbeads.[64] Multicolor fluorescent microbeads made from various polymers and incor-

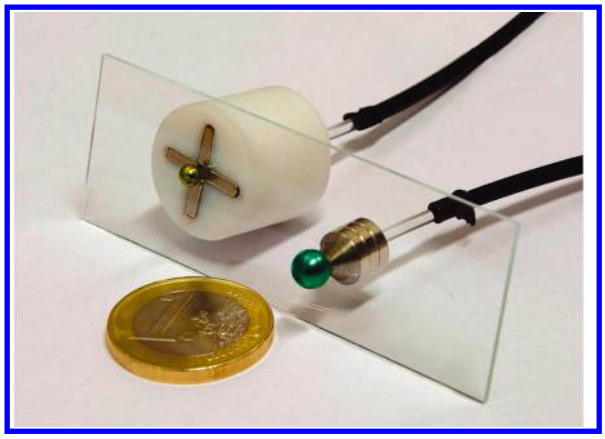

Figure 3. Magnetic sensor macrospheres captured in front of an optical fiber with a radial (left) or axial (right) separator. (Reprinted with permission from ref 63. Copyright American Chemical Society, Washington, DC, 2010.)

porated into a binder polymer resulted in a material whose three signals (for pH, temperature, and oxygen) can be unambiguously assigned after either spectral or time-resolved separation. The respective probes were incorporated into microbeads which prevents FRET from occurring. The material is well-suited for continuous sensing of these parameters in blood or other bioliquids. The multiple sensing and imaging capabilities of optical sensors has been summarized by Stich et al.[12] The measurement of oxygen along with temperature is needed in order to compensate for effects of temperature, since all luminescent probes display more or less temperature-dependent signals. Lo et al.[65] developed a temperature-compensated Stern–Volmer model to eliminate the effects of temperature drift in the range of 25–70 °C. An oxygen-sensitive probe was immobilized in a fluorinated xerogel and deposited on a fiber tip to give a fiber-optic oxygen sensor. The experimental results were fit to the modified Stern–Volmer model to compute temperature compensation coefficients for temperatures between 20 °C and 70 °C.

The use of a luminescent temperature sensor for temperature compensation during oxygen measurement is a more commonly used approach. Fischer et al.[66] used two iridium(III) complexes (of different color) to accomplish dual sensing of oxygen and temperature. One iridium complex is quite sensitive to oxygen and was immobilized in a film of gas-permeable cellulose acetate butyrate. The other complex is sensitive to temperature and was made insensitive to oxygen by encapsulating it into microparticles made from (gas-blocking) poly(acrylonitrile). The phosphorescent signals of both probes can be spectrally separated using optical filters and by luminescence lifetime discrimination. The same group[67,68] later immobilized a luminescent platinum(II) porphyrin probe in core–shell nanoparticles composed of a polystyrene (PS) core and a poly(vinyl pyrrolidone) (PVP) shell, and used an oxygen-insensitive iridium complex in poly(acrylonitrile) microparticles. Both types of particles were dispersed in water (rather than in organic solvents), and the sensor paint was then sprayed onto the object of interest (see Figure 4). The environmentally friendly paints were used to measure barometric pressures in the range of 50–2000 mbar and temperatures in the range of 1–50 °C. The paints can be easily washed away using water.

Oxygen sensors based on the measurement of luminescence intensity are seemingly simple, but the analytical precision often is compromised by fluctuations in the intensity of excitation light,

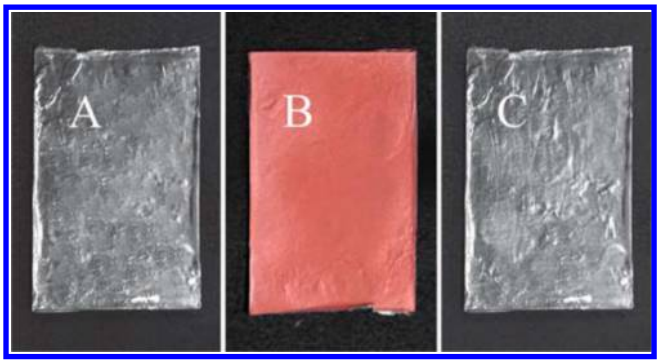

Figure 4. Images of a water-based sensor material deposited on an aluminum foil: (A) before spraying the foils with the PS/PVP particles; (B) after spraying it with the sensor paint (dyed with a red Pt-porphyrin complex), and (C) after removing the red paint with water. (Reproduced from ref 68, with permission of The Royal Society of Chemistry.)

the transmission efficiency of optics, and drifts in the sensitivity of detectors. Ratiometric and lifetime-based sensors have always been considered the remedy for this shortcoming. Chu et al.[69] report on another ratiometric fiber-optic oxygen sensor that is based on a sol–gel matrix doped with two fluorophores. The Pt or Pd complexes with tetrakis(pentafluorophenylporphine) act as the red-emitting oxygen-sensitive probes, while the blue-emitting dye 7-amino-4-trifluoromethylcoumarin acts as the reference dye. This ratiometric sensor has good sensitivity, a response time of ~3 s, and is fully reversible. Effects of spurious fluctuations in the intensity of the excitation source and optical transmission properties of the optic fiber are eliminated.

Oxygen sensors intended for long-term monitoring require luminescent probes that are highly photostable. Fluorinated metalloporphyrins-based oxygen probes have been found to be more photostable and more resistant to oxidation. Borisov et al.[70,71] have synthesized several new fluorinated platinum(II) and palladium(II) benzoporphyrins with extended π-conjugate structure. The photophysical properties and quenching efficiency by oxygen were systematically studied. Results showed that these complexes possess long decay times, good phosphorescence quantum yields, and can be excited with blue or red LEDs. Such fluorinated probes are more photostable, and their emission bands extend to above 800 nm. This is an analytical wavelength that is hardly interfered by background luminescence. The $Ir(ppy\text{-}NPh_2)_3$ complexes represent another group of probes that display exceptional oxygen sensing capabilities and triplet state properties.[72] Strong quenching by oxygen is observed along with a phosphorescence quantum yield of up to 0.7 and a decay time of 4.3 μs in deaerated solution. However, fluorinated metalloporphyrins are more photostable.

Iridium probes usually are photoexcited with blue light. Rather than using conventional light sources, Achatz et al.[73] used upconverting luminescent nanoparticles (UCLNPs) as "nanolamps" to photoexcite an oxygen-sensitive iridium complex. The UCLNPs were first photoexcited by near-infrared laser excitation at 980 nm, and the up-converted blue emission from these nanoparticles is absorbed by the iridium complex whose green luminescence is quenched by oxygen. The UCLNPs exhibit multiple line emissions, some of which may serve as a reference signal, to enable ratiometric readout.

Liquid oxygen is widely used in medical treatment, industry, and propulsion engines, but sensing of liquid oxygen at high pressure and at high flow rates is challenging. Dynamic quenching of luminescence is very strong at high oxygen concentration and therefore is not the method of choice to sense liquids containing oxygen. Here, Raman spectroscopy is superior, as shown by Tiwari et al.[74] who designed an integrated fiber-optic Raman sensor that employs a frequency-doubled 532-nm cw Nd:YAG laser as the light source. A standard spectrometer can be used to collect the Raman spectrum of liquid oxygen or mixtures containing it. The system can also be applied to the detection of liquid nitrogen.

Ammonia. Ammonia is released in large quantities into the environment by the farming industry, by the decomposition of fertilizers, and by (leaky) refrigerators, to mention a few examples. Gaseous ammonia can be sensed via direct IR spectroscopy, but dissolved ammonia cannot be detected and, therefore, is sensed via indicator probes, for example. Gaseous ammonia is in equilibrium with water-dissolved ammonia and ammonium ion, depending on the actual pH of the aqueous phase. Therefore, most sensors for ammonia may also be applied to sense ammonium after proper adjustment of the pH of the sample. Gaseous and dissolved ammonia usually are determined on the basis of its weakly basic character, or its capability of binding to nanocrystalline inorganic materials. A porphyrin-anchored electrostatic self-assembled multilayer was deposited on tapered optical fibers in a thickness of some tens of nanometers for ammonia sensing.[75] The coating was composed of alternate layers of a sulfonated (i.e., anionic) tetraphenylporphine and (cationic) poly(allylamine hydrochloride). Exposure of such a fiber (with a waist diameter of 10 μm) to ammonia induced optical changes in the transmission spectrum. This fiber-optic sensor has a linear sensitivity to gaseous ammonia in the 10–100 ppm concentration range, with response and recovery times of <100 s and ~240 s, respectively. The limit of detection (LOD) is ~2 ppm. Similar sensors were obtained by modifying the fiber cladding with nanometer-thick alternating layers of the same porphine and (anionic) poly(diallyldimethylammonium chloride) or poly(acrylic acid).[76] Such sensors have even lower dynamic ranges (0.1–20 ppm) and short response time. Unfortunately, these sensors are not reversible, but they can be reactivated by washing and drying.

A thin film of polypyrrole (PPy) was doped[77] with various organic and inorganic acids, for example with poly(vinyl sulfonic acid) (PVS), *p*-toluene sulfonic acid, tartaric acid, and acrylic acid. The material was placed, as a cladding, on an optical fiber and tested for response to ammonia. The intensity of light propagating along the sensing region of the multimode fiber was lowered because of evanescent-wave interaction. The effect was most distinct for the PPy–PVS coating. The sensor is slow (response and recovery taking 6 min) but has a low LOD (1–10 ppm at a fiber length of only 2 cm) and gives a stable and repeatable response for up to 32 days.

Thin films of bacteriorhodopsin are sensitive to ammonia[78] in giving a decrease in absorbance at 570 nm and a small increase at 410 nm. This was attributed to the replacement of a water molecule bound to the chromophore by ammonia. The film was coated onto the distal end of an optical fiber to result in a fully reversible FOCS with a linear response in the 10–200 ppm range of ammonia and an LOD of 5 ppm. The response is completely reversible, even though recovery (which is 100 s at up to 100 ppm of ammonia) is long at higher concentrations.

A porous optical fiber was doped with copper(II) chloride to obtain a material for monitoring ammonia in high-temperature gas streams.[79] Ammonia diffuses into the fiber to react with the dopant to form the blue copper–ammonia complex. The concentration of ammonia is proportional to the absorbance at ~550 nm. The reaction is reversible at temperatures up to 450 °C. An LOD of 0.24 ppm (v/v) can be achieved. Moisture (up to 4%) and carbon

dx.doi.org/10.1021/ac303159b | *Anal. Chem.* 2013, 85, 487–508

dioxide (up to 10%) remain inert, but H_2S, SO_2, and NO_2 interfere. Ammonia also binds to nanocrystalline inorganic materials such as zinc oxide (ZnO).[80] When ammonia interacts with the cladding of a fiber modified with ZnO nanocrystals, the intensity of the light propagating along the fiber is weakened, and the output intensity is linearly related to the concentration of ammonia over a wide range. This sensor has good selectivity (for example, over vapors of methanol and ethanol) and reversible response, but response time and recovery are very long (100 and 80 min, respectively). The same group later modified a fiber clad with ZnO doped with Ce^{3+}, Li^+, and Al^{3+} cations.[81] The Ce-doped ZnO exhibited better sensitivity, but most of the other disadvantages have not been overcome.

Ammonia has been sensed via its weak basic character by using acid−base indicators. In addition to the pH indicators used ∼20 years ago, the pH-sensitive dye Oxazine 170 also was shown[82] to give a reversible response. Thin layers of oxazine on a fiber and coated with polydimethylsiloxane (acting as a protective material) undergo a large change in absorbance change at 477 nm after exposure to ammonia. The sensor exhibits a response time of ∼10 s, a low LOD (1.4 ppm), and is fully reversible, but only works for moist gas samples, because water is essential to cause local changes of the pH value. Schmitt et al.[83] developed a similar FOCS for ammonia, using the pH indicator Bromophenol Blue incorporated into matrices of ethyl cellulose or poly(vinyl butyral). The sensor was designed with wireless signal transmission to enable the remote sensing of ammonia in a harsh environment. Fluorescent (rather than absorptiometric) pH indicators also have been employed for quite some time in such sensor schemes. Peng et al.[84] show that eosin also can be used. A microstructured optical fiber was doped with a solution of this pH indicator in cellulose acetate by placing the material in 18 array holes of the microstructure. Fluorescence intensity at 576 nm increases strongly and rapidly (with 500 ms) upon exposure to 50−400 ppm of ammonia. However, the response is not fully reversible, and the indicator must be reactivated by treatment with a solution of hydrochloric acid.

UCLNPs were used by Mader et al.[85] in a new scheme for sensing ammonia. The pH indicator Phenol Red and the UCLNPs (with inner diameters (ids) of typically 50−70 nm) were placed in a polystyrene matrix. The luminescence of the UCLNPs was photoexcited with a diode laser at 980 nm, upon which they emit dual (green and red) luminescence. Exposure of the sensor to ammonia causes an increase in the absorption of Phenol Red (at 560 nm) which, as a result, blocks the green emission of the UCLNPs. The red emission of the UCLNPs, in contrast, remains unaffected and can serve as a stable reference signal. Because of the use of 980 nm as the excitation light source, the optical signal obtained is completely free of background visible luminescence of the sample and of scattered light. This is highly advantageous in the case of sensing ammonia in complex matrices. Similar design has also been used for CO_2 sensing, but using Bromothymol Blue as the indicator (see below).[86] Recall here that the sensing of ammonia via pH-sensitive probes usually is interfered by acidic species such as CO_2, SO_2, NO_x, and vapors of mineral acids and of organic acids such as acetic acid.

Carbon Dioxide. Carbon dioxide (CO_2) is a notorious greenhouse gas and causes global warming. The measurement of CO_2 would be beneficial not only in environmental and meteorology research, but also to the food, beverage, and health industries. CO_2 can be sensed (a) directly via its absorption lines in the IR range, or (b) via the pH changes it causes when reacting with water or weakly alkaline buffers. Chu et al. transferred a known (and clinically used) detection scheme to a new host matrix by immobilizing the pH indicator 1-hydroxy-3,6,8-pyrenetrisulfonate (HPTS) and the base tetraoctylammonium hydroxide in a sol−gel matrix[87] and in a fluorinated xerogel,[88] respectively. Gaseous CO_2 penetrates the membrane, reacts with the base, and thereby causes the inner pH to drop; this, in turn, is indicated by HPTS via a decrease of its fluorescence. Similar sensors were reported[89] that also contain particles of TiO_2 in the sol−gel. The addition of such particles (or of barium sulfate in much earlier sensors) increases the efficiency of photoexcitation, which, in turn, improves the signal-to-noise ratio. It shall be reminded here that the sensing of CO_2 via pH-sensitive probes usually is interfered by basic species such as ammonia and amines, but also by acids much stronger than carbonic acids, for example by vapors of mineral acids and of organic acids such as acetic acid.

A new sensing scheme was introduced[90] that is based on the finding that CO_2 can specifically react with a polymer (referred to as TB-PAM). This interaction results in a change in the polarity near an added polarity-sensitive probe (Nile Red). The probe (which is not pH-sensitive) was dissolved, along with TB-PAM, in an ethyl cellulose matrix. Upon exposure to CO_2, the brick-red color of the sensor matrix changes to magenta, and its fluorescence changes from orange to red. Both gaseous CO_2 (gCO_2) and dissolved CO_2 (dCO_2) can be quantified. The sensor responds to gCO_2 in the range from 0 to 100%, and to dCO_2 in the range from 0 to 1 M solutions of bicarbonate (which is equivalent to a CO_2 partial pressure of up to 255 hPa above the water solution). The LODs are ∼0.23% for gCO_2 and 1.53 hPa for dCO_2. The response times are long (10−25 min, in the case of dCO_2).

Direct IR spectroscopy is the method of choice for sensing gaseous CO_2 down to moderately low concentrations. The gas has two absorption lines (one at 1572.335 nm, the other at 1572.659 nm). Orghici et al.[91] developed a FOCS for dCO_2, using a bare fiber with a coating that selectively extracts CO_2 from an aqueous phase. A single-mode laser diode with an emission wavelength of 1.57 μm served as the light source. The sensor is suitable for online and in situ monitoring of CO_2 in both gas phase and in fluid phase, partially by evanescent-wave interaction. Unfortunately, analytical ranges and LODs were not indicated in the article. Evanescent-wave sensors for CO_2 exhibit lower LODs than conventional absorptiometric sensors because of a large number of total reflections that occurs at the (bare) core of an optical fiber while the light beam is conveyed through it. The implementation of waveguiding nanostructures[92] can further improve the response to gases such as CO_2.

Nitrogen Oxides. Atmospheric nitrogen dioxide and ozone are notorious pollutants of air. Atmospheric NO_2, ozone, and RH can be simultaneously determined[93] with a FOCS probe whose color-forming element comprises a transparent silica gel support impregnated with the reagent 8-amino-1-naphthol-5-sulfonic acid (ANS). The ANS on the plate reacts with NO_2 and O_3 to form brown- and pink-colored products, respectively. The transmission of the support changes reversibly from the visible range to the NIR range as a function of the RH around the plate. The LODs are 0.64 and 0.42 ppb (v/v) for NO_2 and O_3, respectively, thereby providing a viable approach for inexpensive (but irreversible) probing of atmospheric NO_2 and O_3. The same group[94] later used 1,3-alternate O-hexylcalix[4]arene as a receptor molecular for sensing NO_2, but the LOD is about the same. Ding et al.[95] fabricated a fiber-optic sensor for dissolved NO based on the fluorogenic (but irreversible) reagent diaminobenzoacridine

dx.doi.org/10.1021/ac303159b | Anal. Chem. 2013, 85, 487−508

which was immobilized in a film of cellulose acetate. Fluorescence intensity and NO concentration are linearly related in the 1.8−9.0 μM concentration range.

Nitric oxide has a far-UV absorption band at 191 nm. This can be used for fiber-optic monitoring of nitric oxides in exhaust gas.[96] The LOD is as low as 5 ppm, the response time is 3.4 s, but many gases and vapors (for example of gasoline) are likely to interfere, because of their own absorption bands in this spectral range. No sensors for NO_x that would exploit the IR absorption of the various NO_x species have been reported in the time covered in this review.

Vapors of Organic Solvents. Vapors or organic chemicals, often referred to as volatile organic compounds (VOCs), are sensed by optical means mainly in order to reduce the risk of explosion that is associated with electrochemical sensing schemes. Among the various VOCs, alcohols and gasoline have attracted the most interest. Alcohols are widely used in industry, as additives to gasoline, as energy sources in fuel cells, and, of course, in various drinks. One large market for respective sensors is in the quantitation of alcohol in breath air. FOCSs for alcohols can be small, simple, and portable. A polypyrrole (PPy)-conducting polymer was identified[97] as a material that is sensitive to vapors of methanol and ethanol, and this resulted in a respective fiber-optic reflectance sensor. It exhibits reversible response, for example, from 1 to 300 ppm (v/v) of methanol. An organometallic compound of formula $[Au_2Ag_2(C_6F_5)_4(C_{10}H_{14})]_n$ immobilized in a microporous xerogel served as the optical probe in an FOCS for vapors of methanol and ethanol.[98] The compound, a red powder, shows yellow fluorescence with a peak at 585 nm if photoexcited at 380 nm, and it undergoes large changes in color if exposed to various VOCs. Its reflectivity exponentially depends on vapor concentration of up to 6 mM of methanol and up to 3 mM of ethanol. The response, which is fully reversibly, is attributed to changes in the refractive index (RI) of the compound. The response time is 2−4 min for vapors of methanol, and 6−10 min for those of ethanol, and the respective LODs are 1.65 mM and 0.83 mM. The same group[99] later placed the organometallic compound on Fabry−Perot nanocavities to fabricate an optical fiber sensor for vapors of ethanol and with a much-shorter response time (36 s).

The strong fluorophore Rhodamine 6G was doped[100] into a TiO_2 film, which then was deposited on a clad of an optical fiber. The response of this material is due to an increased absorption of the evanescent wave when the sensing film interacts with vapors of alcohols to form a colored product. The difference between the output power in the presence and absence of vapor is a measure for its concentration. The sensor works over the concentration range of 0−10 000 ppm.

Inorganic nanocrystals not only bind ammonia (see above), but also vapors of alcohols. Nanoparticles made from SnO_2 and SnO_2:CuO were used[101] to modify the cladding of a fiber to obtain a FOCS for ethanol that can be operated at room temperature. The RI of the modified cladding changed with exposure to ethanol, and the sensor based on the use of SnO_2:CuO has a 3-fold better sensitivity for ethanol, compared to the one made with SnO_2. The group[102] also proposed an optical fiber sensor for vapors of ethanol, where the conventional cladding was replaced by $Zn_{1-x}Cd_xO$ (x = 0.00−0.10) nanorods.

Single-walled carbon nanotubes (SWCNTs) are another nanomaterial sensitive to VOCs. A poly(methyl methacrylate) optical fiber wrapped with SWCNTs was found[103] to respond to ammonia, ethanol, and methanol vapors at room temperature at levels of 0−500 ppm by a change in its absorption at 678 nm. The relative signal change is quite small, being only 180 counts at 500 ppm of ammonia over a background of 3440 counts. Sensors with thin films of SWCNTs are said to respond better to ammonia, while thick films prefer alcohols. Cusano et al.[104] explored analyte adsorption on SWCNTs to construct a sensor for VOCs that displays opposite responses upon exposure to electron-donating (xylene and ethanol vapors) or electron-accepting (NO_2) analytes. However, the selectivity of such sensors is poor, and certain gases may annihilate the response to others. Graphene (a nanomaterial chemically related to SWCNTs) was applied in a FOCS for acetone vapor.[105] Sensing relies on the variation of the reflectance of the sensitive layer due to adsorption of vapor on the graphene film. Acetone in concentrations from 44 ppm to 352 ppm is reversibly detectable, but the selectivity is poor. Note that, at this stage, selectivity is not always needed. In fact, there is also a need for sensors that respond to *all* types of VOCs.

Nanoporous anodic aluminum oxide (AAO) coated with a thin film of gold was used[106] for reflective interferometric sensing of volatile sulfur compounds and gaseous hydrogen sulfide (H_2S). The adsorption of thiols on gold films causes a shift in the fringe pattern of the Fabry−Perot interferometer. The sensor displays a linear response to H_2S at levels of 0%−2%. The known effect of gaseous hydrochloric acid and butylamine (a weak base) on polyaniline was exploited[107] to construct respective fiber-optic sensors. Hydrochloric acid causes an increase in signal intensity, whereas butylamine (and other amines) causes a decrease. Response times range from 0.5 min to 1 min, but the back reaction (as far as specified) is as slow as in the case of non-fiber-optic sensors, and the analytical range typically is 400−4000 ppm (v/v). The selectivity of such sensors obviously is poor.

SENSORS FOR HUMIDITY, WATER FRACTIONS, HYDROGEN PEROXIDE, AND HYDRAZINE

Humidity. Optical humidity sensors have numerous applications, examples being the chemical industry, aviation, climate research, and food technology. Fiber-optic sensing of relative humidity (RH) was demonstrated[108] with a twin low-coherence Sagnac interferometer that consists of two interferometers with twisted highly birefringent fibers. The first was used for a dry-bulb measurement of temperature, the other for the wet-bulb temperature. The uncertainties for temperature and RH are better than 0.01 °C and 4%, respectively. Another fiber sensor for RH was reported[109] that is based on a Fabry−Perot interferometer. A fiber was coated with a thin layer of the moisture-sensitive biopolymer chitosan. RH causes swelling of the chitosan film, which induces optical path modulation on the order of nanometers. The sensitivity typically is 0.13 nm per % RH in the range from 20% to 95%, and the response time is as low as 380 ms. Nanocrystalline zinc oxide also was employed to sense RH. It was deposited[110] on a U-shaped glass substrate that acts as a waveguide. The optical permeability is a function of RH in the range from 5% to 90% and decreases linearly with an increase in RH. Response and recovery occur within <35 s. Similarly, TiO_2 particles were used to sense very low levels of RH in the facilities of European Organization for Nuclear Research (CERN).[111] The RH values determined with the optical fiber sensor agreed well with those of common hygrometers both at 20° and 0 °C, with limits of detection for RH regimes of <0.1%. Akita et al.[112] fabricated a humidity sensor with a heterocore optical fiber structure that was coated with a nanolayer of the hygroscopic polymeric amino acids poly(glutamic acid) and polylysine. The RI of the polymer layer varies with RH around the sensor. This induces the light intensity to change while

dx.doi.org/10.1021/ac303159b | Anal. Chem. 2013, 85, 487−508

conveyed through the fiber. The sensor measures RH values between 50% and 93%, with a response time of ~400 ms.

Even a conventional LPFG coated with a thin film of plain silica nanospheres works as a sensor for RH.[113] The coating changes its optical properties on exposure to various levels of humidity and this results in a shift of the resonance wavelength of the fiber grating by up to 12 nm in an RH range of 20%–80% while being virtually insensitive to temperature. A similar approach had been reported by Estella et al.,[114] who used a porous silica xerogel film as the sensing element. Atmospheric gases or vapors do not interfere, and the sensor can detect RHs between 4% and 100%, with response times between 10 s to <2 min. Zhao et al.[115] developed a low-cost fiber-optic humidity sensor using a similar material (silica sol–gel) deposited as a thin film on a U-bent optical fiber and doped with Methylene Blue dye. The logarithm of the absorbance is linearly related to RH in the range from 1% to 70%. Løkken[116] has compared the performance of several hygrometers for monitoring RH in natural gases and in the presence of methanol. Methanol vapor does not affect these hygrometers as long as its concentration is below 10 μmol/mol. At high levels of methanol (170 and 750 μmol/mol), all sensors were affected, except for the fiber-optic sensor.

Water Fractions. Sensing the fraction of water in industrial solvents, in various types of fuel and in alcoholic drinks, is of obvious significance. Existing methods are far from being perfect with respect to speed, flexibility, and precision. Solvatochromic probes of all types (from the visible to the IR, in absorption, reflection, and fluorescence) are known but can be used for discrete samples (in cuvettes, for example) only, but not for repeated or continuous sensing. Spectral interrogation was used[117] in an SPR-based fiber-optic sensor for the detection of low water fractions (1%–10%) in ethanol. The resonance wavelength varies linearly with the water fraction in this range, with a shift of 1.149 nm per % water. The sensor has a resolution of 0.145% water, which is better than the evanescent-wave absorption sensor reported in a similar study. Water, being a (weak) IR absorber, can be determined via its IR absorption at low levels in mixtures with ethanol.[118] Evanescent field absorption spectroscopy and a coiled fiber-optic system were applied. Principal component regression and classical least-squares models were used to build the calibration model. The standard errors of predictions of water fractions in ethanol are 3.2% and 0.42%, respectively.

Hydrogen Peroxide and Hydrazine. H_2O_2 is an important industrial chemical and the product of enzymes out of the group of oxidases. The titanium complex with acetylacetonate (like other titanium compounds) is known to react with H_2O_2 to form a yellow product. This reaction was exploited[119] to develop a FOCS by immobilizing the complex in a Nafion coating on an optical fiber. H_2O_2 presented in an aqueous solution can diffuse into the polymer coating to form a product with peak absorption at 360 nm, which is detected via evanescent-wave absorption spectrometry. The sensor is reversible and has an LOD as low as 7.4×10^{-8} mol/L, which makes it a viable tool for use in membrane fuel cells. Hydrazine also was detected with a chromogenic reaction.[120] A silica core optic fiber cladding was replaced by a pentacenediquinone-type of polymer that gives a red coloration with hydrazine.

SENSORS FOR pH VALUES, IONS, AND SALINITY

This section covers sensors for all types of inorganic ions, including the proton (i.e., pH), cations, and anions. Optical sensing of pH remains to be of great interest, even though all optical sensors suffer from cross sensitivity to ionic strength. However, the number of articles on pH sensors is decreasing, which does not come as a surprise in view of the state of the art and the fact that FOCS for pH are commercially available. On the other side, sensing of pH values of <1 and >12 still represents a substantial challenge in terms of materials science. Optical pH sensors respond over a limited range of pH only (in most cases). It also needs be stated that (i) many pH sensors presented in the past few years are (minor) modifications only of previously reported sensing schemes and materials, and (ii) authors often do not properly cite previous work on the subject. In the worst case, sensors are presented that are inferior to others described before. Such sensors are not treated here.

pH Values. Two methods are most common. The first uses materials that swell as a function of pH value, and the other is based on the use of optical probes (indicators). Sensing pH by making use of polymers that swell as a function of pH have attracted substantial interest, because such materials are potentially quite stable over time and because indicator probes (that tend to bleach, decompose, or leach) are not needed. The state of the art in this field has summarized by Richter et al.[121] Figure 5 shows how hydrogel polymers (the preferred group of materials) can swell, then undergo phase transitions, as a function of the actual pH value.

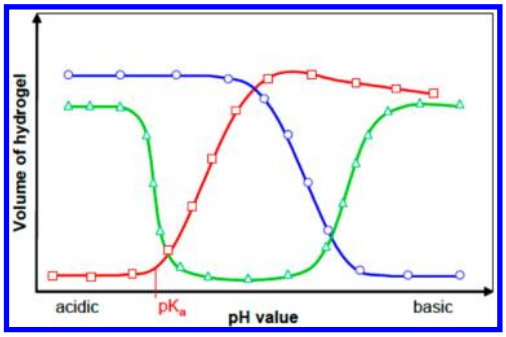

Figure 5. Phase transition behavior of polyelectrolyte hydrogels. Acidic hydrogels (denoted by the red trace) are ionized by deprotonation in basic solutions, which have an excess of hydroxyl groups. Basic hydrogels (denoted by the blue trace) swell in acidic solutions due to the ionization of their basic groups by protonation. Amphiphilic hydrogels (denoted by the green trace) contain both acidic and basic groups and therefore can undergo two phase transitions. (Reprinted with permission from ref 121. Copyright VCH, Weinheim, Germany, 2007.)

Swellable materials were also used[122] in fiber-optic pH sensors based on modal interferometry of self-assembled polyelectrolyte coatings. These were deposited by the layer-by-layer electrostatic self-assembly technique on the side surface of a thin-core fiber modal interferometer (TCFMI). The RI of the alternating poly(allylamine hydrochloride) and poly(acrylic acid) nanocoating is reversibly modulated by swelling and deswelling due to varying local pH values. The corresponding RI of the interface layer can be precisely determined by the TCFMI. The sensor has a rise time of 120 s and a fall time of 200 s, and it covers the pH range of 2.5–10 with a resolution of 0.013 pH units. This is better than most indicator-based optical pH sensors. In related work,[123,124] other negatively charged and positively charged polyions were used, which reduced the response time to <20 s. The same group[125] also introduced two biocompatible polyelectrolytes (sodium alginate and polyethylenimine) as coatings for constructing a highly biocompatible pH sensor. The sensor

dx.doi.org/10.1021/ac303159b | Anal. Chem. 2013, 85, 487–508

exhibits a linear, fast (rise time 60 s, fall time 80 s), and reversible response over a large pH range (2−11) with a resolution of <0.01 pH units. This makes it precise enough for clinical pH measurements.

The second approach to sense pH values (based on pH-sensitive indicators) was realized[126] in an evanescent-wave sensor with wide analytical range. A mixture of the three pH-sensitive indicators (Cresol Red, Bromophenol Blue, and Chlorophenol Red) was immobilized on the unclad surface of a fiber core, using a sol−gel cladding technology. The resulting sensor gives a linear and reversible response over the pH range of 4.5−13.0. Bromocresol Green and Cresol Red were also used in a mode-filtered fiber-optic pH sensor, where the optical fiber is inserted into a fused-silica capillary coated with the pH indicator.[127] The Bromocresol Green-based sensor measures pH values between 2.0 and 8.0, and the Cresol Red sensor measures pH values between 9.0 and 13.0; both response times were within 120 s. Among the fluorescent pH probes, fluorescein is quite common, even though it is not very photostable. pH-sensitive fluorescent dyes and their applications in fiber-optic sensors, in in-vivo sensing and imaging, and in planar film-based sensing and imaging have been reviewed.[128] However, numerous other pH probes are conceivable. Khan et al.[129] doped 1-(2-pyridylazo)-2-naphthol in a silica sol−gel film and coated the film onto the distal end of an optical fiber to obtain a sensor for the pH range of 7.2−8.4, which encompasses the clinical-relevant range. Other fluorescent pH probes include (a) a polymerizable piperazinyl-1, 8-naphthalimide (for the pH range of 6.8−8.0),[130] (b) various near-IR fluorescent pH indicators of the boron-chelated tetraarylazadipyrromethane type[131] (with a response based on photoinduced electron transfer, absorption maxima between 660 and 710 nm and fluorescence emission maxima at 680−740 nm, molar absorption coefficients of 80 000 M^{-1} cm^{-1}, quantum yields of up to 20%, and analytical ranges between 7 and 11), and (c) certain fluorescent Schiff bases[132] (working in plasticized PVC and over pH ranges of 2.0−7.0 and 8.0−12.0, respectively; full reversibility, and response times of <1 min).

Photon upconverting luminescent lanthanide nanorods were used by Sun et al.[22] in a new type of pH sensor. The nanorods, upon illumination with a 980-nm diode laser, display visible luminescence. They were incorporated along with the pH indicator Bromothymol Blue (BTB) in a hydrogel matrix. The red luminescence of the nanorods is reabsorbed by BTB at alkaline pH values where BTB is blue. However, being yellow at acidic pH values, BTB does not cause a strong inner filter effect at pH values below 8. The sensor responds to pH values between 6 and 10 within less than 30 s. Its long-wave excitation and emission are said to make the sensor well-suited for sensing pH, in even strongly colored biomatter and in deeper regions of tissue.

Luminescence lifetime-based sensing of pH can prevent signal fluctuations due to instrumental effects and varying sample background, since lifetime is an intrinsic parameter that is dependent only on the microenvironment of the luminescent probe. However, many luminescent pH indicators have lifetimes of <10 ns, which causes a substantial instrumental effort, in terms of precise determination. In addition, luminescence background cannot be eliminated by time gating. This situation can be overcome using dual-lifetime referencing (DLR) or long-lifetime probes. DLR enables the pH to be determined by measuring the phase shift or the overall apparent lifetime (in units of μs), as a function of pH.[133] The method often is performed with sensor nanoparticles (e.g., for pH), and signals are measured relative to the (long-lived) luminescence of an inert reference luminophore out of the group of metal ligand complexes. The pH-sensing properties of pH-sensitive nanoparticles were fine-tuned by varying the substituents of pH indicators,[134] and the inert and long-lifetime reference luminophore can serve as the optical information on the local temperature.[135]

pH probes with long luminescence lifetime are not very common. Goncalves et al.[136] synthesized long-lifetime ruthenium complexes that are viable indicators for fiber-optic lifetime sensing of pH. Their luminescence intensities and excited-state lifetimes all show a typical sigmoidal variation with pH in the pH range of 3−9, and typical lifetimes in the microsecond range, which can be fairly easily determined and also allow for suppression of background by performing time-resolved spectroscopy.

In a completely different approach, pH values were determined via SPR of a film with a silver nanostructure.[137] The film was fabricated by thermolysis and exhibits a strong localized SPR at ∼400 nm, whose spectral position is sensitive to pH. The silver nanoparticles were placed in a matrix of poly(vinyl alcohol), and the sensor thus obtained works in the pH range of 3.6−9.3. The material was deposited both on tapered and nontapered U-bent optical fibers, with the former performing much better.

Ions. Metal ions play important roles in body fluids, environmental issues, and safety control of products. Sensing light metal ions such as sodium, potassium, calcium, and magnesium plays big roles in blood testing ("blood electrolytes"). Such sensors, in the form of planar sensing elements, are quite established and commercialized but not in the form of fiber-optic sensors. Sampling and sensing at sites other than the artery are gaining much interest. A FOCS for sensing potassium in tear fluid (shown in Figure 6) was reported[138] that makes use of the

Figure 6. (A) Flat-ended optical probe used in an ex vivo lens assay. (B) Straight fiber-optic probe for direct assay in tear fluid in the lower meniscus. (Reproduced from ref 138, with permission from Elsevier.)

displacement of sodium from water-soluble sodium tetraphenyl borate by the K^+ ion to form insoluble potassium tetraphenyl borate. The resultant white precipitate is dispersed in a water-swollen hydrogel film, where it causes incident light to be scattered. This is detected via a fiber-optic system. A linear relationship does exist between the signal loss and the potassium concentration in the range of 1−8 mg/mL. Examples are given for the quantitation of K^+ ions in an ex vivo contact lens. The acceptance of such sensors by users should be forthcoming.

Lumogallion is a well-established molecular probe for the Al^{3+} ion. A chemically modified lumogallion was attached to the surface of an optical fiber[139] by covalent attachment to a polyelectrolyte that was deposited in the internal holes of a suspended-core

dx.doi.org/10.1021/ac303159b | Anal. Chem. 2013, 85, 487−508

microstructured fiber-optic waveguide. The sensor undergoes a large fluorescence enhancement in the presence of the Al^{3+} ion, which is detected by evanescent-wave photoexcitation and enables the Al^{3+} ion to be sensed in real time and at sensing sites distributed over a wide distance. The LOD is moderate (100 μM concentrations), and, as expected, Ga^{2+} and In^{2+} ions interfere. A fiber-optic biosensor was reported for rapid screening of milk for Cd^{2+} ions.[140] It consists of entire *Bacillus badius* cells, along with the pH indicator probe Phenol Red as an indicator, both immobilized onto circular plastic disks in sol–gel membranes. The *Bacillus badius* possesses a highly active urease whose activity is inhibited by Cd^{2+} ion. This resulting lack of pH changes is reported by the indicator. An LOD of 0.1 μg/L of Cd^{2+} has been achieved with a sample volume of 10 μL. The biosensor can be stored for 90 days at 4 °C in a 10% solution of glycerol in water. Other inhibitors are likely to interfere but also are not supposed to be present in milk. Cd^{2+} ion was also detected[141] with a transmission-based localized SPR fiber-optic sensor. It was constructed by immobilizing phytochelatins of the type $(Glu\text{-}Cys)_n$-Gly on an Au-nanoparticle-modified optical fiber. The absorbance of the sensor increases by up to 9% upon increasing the Cd^{2+} ion level from 1 ppb to 8 ppb, with a sensitivity (slope) of 1.24 ppb^{-1} and an impressively low LOD of 0.16 ppb. The sensor retained 85% of its original activity after nine cycles of deactivation and reactivations. Reproducible results were still obtained after storage in a 5% trehalose solution at 4 °C for 35 days. The same group[142] also reported the immobilization of certain monoclonal antibodies instead of phytochelatins to give a sensor for Pb ions, with an analytical range between 10 ppb and 100 ppb and an LOD of 0.27 ppb.

The highly toxic Hg^{2+} ion was detected[143] via a thin film of silver-doped zeolite ZSM-5. Interacting with Hg^{2+} results in a change in the RI of the film. The change in the intensity of reflected light is related to the concentration of Hg^{2+} ions in the 1–10 ppm range, with an LOD of 1 ppm. Most metal ions do not interfere, but the sensor is unlikely to be reversible (similar to practically all sensors of that type). In another fiber-optic sensor for the Hg^{2+} ion,[144] the authors have coated a thin-core fiber modal interferometer with an ultrathin film of alternating layers of poly(*N*-ethyl-4-vinylpyridinium chloride) (P4VP) and poly(sodium-*p*-styrenesulfonate) (the so-called "layer-by-layer" technique). The attraction between the soft base P4VP and the soft acid $[Hg(Cl)_4]^{2-}$ causes a change in the RI of the nanocoating, and this was detected by the interferometer. This sensor is highly selective for the Hg^{2+} ion; its LOD and response time are 1 nM and 30 s, respectively. A reusable evanescent-wave biosensor for the Hg^{2+} ion was developed[145] that relies on a direct structure-competitive detection mode. A DNA probe was covalently immobilized on an optical fiber, and a fluorescently labeled complementary DNA was first hybridized to it. If exposed to Hg(II), the DNA probe that comprises a sequence of T–T mismatch pairs specifically binds to the metal ion to form a $T\text{–}Hg^{2+}\text{–}T$ complex by folding the DNA segments into a hairpin structure. The fluorescently labeled complementary DNA will be released into solution, and, in turn, will cause a decrease of fluorescence intensity of the fiber-optic system. The sensor displays a very good LOD of 2.1 nM and high selectivity. Although the response is irreversible, the surface of the probe can be regenerated with a 0.5% solution (pH 1.9) of the detergent SDS. The probe was used 100 times with no significant loss in performance.

Divalent lead (Pb^{2+}), which is another heavy-metal pollutant, was detected[146] with an optical fiber reflectance sensor, based on the well-known probe 2,7-bis(2-arsenophenylazo)1,8-dihydroxynaphthalene-3,6-disulfonate immobilized on ion-exchanger beads. The reflectance of red light at 665 nm served as the analytical signal, and the Pb^{2+} ion was sensed up to 21 ppm levels with an LOD of 0.01 ppm. The sensor can be regenerated with 0.1 M nitric acid and was specifically used to quantify lead in gasoline after ashing, but is not specific. In another approach for sensing Pb(II),[147] the chromogenic reagent dithizone was immobilized on a support to give a sensor material that enables self-referenced reflectance-based sensing. It works in the concentration range of 0.5–30 ppm with an LOD of 500 ppb and can be regenerated with 0.1 M solutions of strong acids within 2 min. However, dithizone is poorly selective. Both these sensors are more suitable for sensing the total heavy-metal ions, which will be discussed later. Uranyl ion can be detected by fiber-optic photometry via formation of its chelate complex with dihydroxyisoamethryin.[148] The chelator, when tethered to a fiber surface, changes its color upon binding to uranyl ion, which allows it to be detected at 50–100 ppb levels with very good selectivity.

Rather than sensing single (polluting) ions, there is a tendency to determine the total concentration of heavy-metal ions (tHMs) in water samples. This parameter can be quickly determined with a thin-core fiber modal interferometer having a nanocoating that is self-assembled on its surface via the LbL technique.[149] Specifically, poly(4-vinylpyridine) and poly(acrylic acid) were deposited in this way. Immersed into solutions containing metal ions, the RI of the nanocoating on the sensor is changed because of the interaction of HM ions with the coating. The concentration of tHMs can be determined by measurement of the dip wavelength of the transmission spectrum. The sensor is reusable and has a fast response over a wide total concentration range (from 10 nM to 0.1 M). The quenching of the luminescence of upconverting luminescent nanoparticles (UCLNPs) by heavy-metal ions is exploited in other respective sensors.[150] The UCLNPs consist of hexagonal $NaYF_4$ nanocrystals doped with trivalent rare-earth ions, and quenching was studied for the Cu^{2+}, Hg^{2+}, Pb^{2+}, Cd^{2+}, Co^{2+}, Ag^{+}, Fe^{3+}, and Zn^{2+} ions, and for the Br^{-} and I^{-} anions. It was found to be particularly strong for Hg^{2+} ions. Both static and dynamic quenching does occur. The UCLNPs display two main emission bands (in the blue, green, red, or near-IR part of the spectrum), and the quenching efficiencies for these bands are different. However, the method is not highly sensitive. The activity of urease is inhibited by many HM ions, and this can be explored for determined tHMs in aqueous samples.[151] The respective fiber-optic biosensor consists of a sol–gel film containing urease and chlorophenol red. In the presence of heavy-metal ions, the reduced enzyme activity causes a much smaller color change of the indicator, and its absorbance at 580 nm can be related to the concentration of HM ions. A linear calibration curve of heavy metals against the percentage inhibition of urease was obtained at the microgram per liter (μg/L) level, and the biosensor can be regenerated using the complexing agent EDTA. Also see the closely related work in ref 140 presented earlier on cadmium(II) in milk.

FOCS for anions are less common. Fluoride was determined[152] by two absorption-based sensors (a light-emitting-diode-based sensor and an evanescent-wave fiber-optic sensor) that rely on the principle that the F^{-} ion can react with zirconium-dye complexes to mask the Zr(IV) ion to form a colorless complex anion (ZrF_6^{2-}) and the free (less-colored) dye. As a result, absorbance decreases with increasing fluoride concentration. The sensors cover the 0–3.0 ppm range, which is the one that can occur in

dx.doi.org/10.1021/ac303159b | *Anal. Chem.* 2013, 85, 487–508

drinking water in certain countries due to (intended) addition of fluoride. Nguyen et al.[153] developed a fiber-optic chloride sensor based on the fluorescence quenching of an acridinium dye, and this sensor can detect chloride at concentrations of >0.1 M. Similar to the long-known planar sensor using the same chemistry and applied in clinical serum analyzers, the sensor also responds to bromide and iodide.

Salinity and Ionic Strength. Sensors for salinity and ionic strength are needed in marine sciences (for example, to study water in estuaries), during blood dialysis, and in the chemical and nuclear industry in general. The RI of salt water changes as a function of its salinity. Thus, most fiber-optic sensors for salinity and ionic strength are based on the measurement of changes in RI. A tapered plastic multimode fiber-optic sensor for the continuous monitoring of salinity was reported[154] that exploits the increment in the transmission of the sensor when immersed in highly concentrated solutions of sodium chloride with its RI that is different from that of plain water. As the concentration of sodium chloride increases from 0% to 12%, the output voltage of the sensor increases linearly from 0.109 mV to 1.142 mV with a sensitivity (slope) of 0.0024 mV per 1% of sodium chloride. The use of plastic multimode fiber made the sensor tougher and easy to fabricate and handle. Possetti et al.[155] compared an LPG-based interferometer for salinity to an Abbé refractometer within the salt concentration range of 0−150 g/L. The fiber-optic refractometer has a resolution that is ∼2 times better than that of the Abbé instrument. However, the fiber-optic sensor is more sensitive to thermal fluctuations. Salinity also was measured with a differential refractometer[156] where beam deviation (caused by changes in salinity) is detected with a fiber-optic array and recorded by a charge-coupled device. The sensor works in the salinity range of 0%−4.5%, and the effects of temperature were largely reduced due to the dual beam technique applied.

SENSORS FOR ORGANIC SPECIES

This chapter covers sensors (but not biosensors) for organic species such as explosives, pollutants, agrochemicals, nerve agents, drugs and pharmaceuticals, gasoline, and oil. FOCS have wide potential applications in these fields because of their compact size. In fact, several portable devices have been developed for quick, quantitative and, partially, real-time analysis. Trace quantities of oil in (sea)water most often originate from the improper disposal of machine oils. A mid-infrared (MIR) evanescent-field fiber-optic sensor has been described.[157] An MIR-transparent silver halide optical fiber was applied to interrogate oil-in-water emulsions via the evanescent field emanating from the waveguide surface and penetrating its environment by a couple of micrometers. Unmodified fibers and fibers surface-modified with grafted epoxidized polybutadiene layers enabled the direct detection of crude oil in a water matrix at the ppm-to-ppb concentration level. Thus, direct chemical sensing of IR signatures of raw oil without any sample preparation and at levels of down to 46 ppb was achieved, with a response time of a few seconds.

A low-cost, high-performance detector for the explosive trinitrotoluene (TNT) in the vapor phase utilizes a multimode fiber sensing system.[158] It is based on the quenching of the luminescence of a fluorescent polymer by TNT. The sensor has a 10-s response time at a level of 30% quenching. Nauyen et al.[159,160] presented a fiber-optic sensor for cocaine detection based on a fluorescent molecularly imprinted polymer (MIP). A fluorescein moiety serves as the signaling reporter in the MIP that was covalently attached to the distal end of an optical fiber. The fluorescence intensity of the sensor increased in response to exposure to cocaine in the concentration range from 0−500 μM in aqueous acetonitrile solution with good reproducibility over 24 h. However, aqueous acetonitrile was used as the solvent, which made the sensor hardly useful for drug detection in the human body.

The RI of polypyrrole films doped with 1,5-naphthalenedisulfonate is altered by adsorption of phosphonates such as dimethyl methylphosphonate.[161] The film was deposited as a cladding on multimode optic fibers, and the adsorption of phosphonates on the films causes a change in the intensity of transmitted light. The sensor can detect 134 ppm of dimethyl methylphosphonate and has good thermal and environmental stability. While not specific for specific phosphonate, the sensor does not respond to species such as ammonia, acetone, methanol, or water.

Acetic acid was sensed[162] with an interferometric fiber-optic sensor based on a FBG Fabry−Perot cavity that was coated with a thin film of a composite made from sol−gel and poly(vinyl pyrrolidone). The wavelength of the interferometric peak changes with the concentration of acetic acid (and, probably, other carboxy acids). Coupled to a commercial modulated interferometer, the FOCS can detect acetic acid with a sensitivity (slope) of 1° per 0.01% of acid, and with a resolution of 0.2% (v/v). The compound *p*-aminophenol (a metabolite of a pain drug that can occur in wastewater) was sensed[163] with an optical fiber reflectance sensor. The sensor chemistry is composed of a tetrahydroxycalix[4]arene (CAL4) immobilized on an XAD-16 ion exchanger in a solid matrix. The reaction of *p*-aminophenol with CAL4 in the presence of an oxidant produces a blue indophenol dye whose reflectance is measured at 620 nm. The sensor can detect *p*-aminophenol at 0.5−35 ppm levels, with an LOD of 0.1 ppm and a response time 5 min, but acts irreversibly and responds to other aminophenols.

Fiber-optic (micro)sensors for glucose have been regarded as one of the most desirable devices in this field, because they are urgently needed in the treatment of diabetes mellitus, based on an artificial pancreas. In most cases, glucose is sensed via an enzymatic reaction (see the next section on Biosensors), but nonenzymatic methods have been reported more recently. Sensors such as the one reported by Binu et al.[164] (based on variations in the RI of aqueous solutions of glucose in distilled water) are not suitable for that purpose, because they do not display any selectivity. A substantial improvement is accomplished by placing a carbohydrate-sensitive hydrogel at the end of optical fiber that acts as a Fabry−Perot cavity.[165] Glucose-sensing capability is introduced by incorporating boronic acid groups into an acrylamide-based hydrogel, as summarized in a review.[166] The interaction between glucose and boronic acid induces swelling and a change in the length of the gel that can be detected by interferometry. The signal change at a level of 2.5 mM glucose is −1760 nm per mM. Selectivity is a big issue in boronic acid-based sensors, but in this case, mannose, sucrose, fructose, and galactose only displayed a response of ∼10% of that of glucose.

Libish et al.[167] developed a fiber-optic sensor for detecting the adulteration of edible oils. An LPG was used and it was found that both the location of the resonance peak shifts and its amplitude changes due to changes of the RI of the oils. At optimized conditions, the LOD of adulteration can reach 3% for a binary mixture of coconut oil and paraffin oil, and 4% for sunflower oil and paraffin oil binary mixtures. However, the sensor is hardly to be calibrated, and any change of oil composition is likely to alter the results, to a large extent. The composition (and thus the chemical properties) of wine grapes steadily change during ripening,[168] and the quantification of saccharidic constituents

dx.doi.org/10.1021/ac303159b | *Anal. Chem.* 2013, 85, 487−508

were studied[169] using NIR fiber-optic sensors that can be regarded as a miniaturized FTIR spectrometers. Given the complexity of such data, mathematical models, chemometrics, and PLS must be applied. At the end, such sensors can provide abundant information on food process monitoring, quality control, and safety control. The same technique also found its application in the identification of wall paintings.[170]

BIOSENSORS

This section covers biosensors based on the use of antibodies, nucleic acids, aptamers, enzymes, and even entire cells. Biosensors make use of biological components in order to sense a species of interest (which, by itself, need not be a "biospecies"). On the other side, chemical sensors not using a biological component but placed in a biological matrix (such as a pH electrode in blood) *are not biosensors* by definition. Note that some of the biosensors can be found in other chapters (for example, on organic species or metal ion sensors) if this was deemed to be more appropriate.

The adsorption of proteins on nanofilms is difficult to detect by conventional means. A Fabry–Perot interferometric fiber-optic method was reported that enables such a process to be easily studied.[171] The membrane was built up by alternatively depositing layers of (cationic) chitosan and (anionic) poly(styrene sulfonate) by the LBL technique. Protein adsorption was monitored via the shift in the interference pattern. The method offers better dynamic range and stability compared to certain other detection methods but is not selective at all.

Immunosensors. The interaction between antigen and antibody is known for its high affinity and specificity but is virtually irreversible so that fiber-optic "immunosensors" are better referred to as immunoprobes. ELISA type of immunoassays can involve several working steps and can be slow. A solution assay for ricin toxin (via recognition of a substitute of its A chain subunit) was worked out and converted[172] into a fiber-optic assay. The (commercial) fiber-optic biosensor system called "Raptor" served as the detection platform. Polyclonal antiricin antibody was captured on the waveguide through incubation. Four waveguides were assembled into each coupon, to enable multiplexed assays in one run. Fluorescently labeled antibody was used as the detector antibody and resulted in LODs of 10 and 60 ng per mL, respectively, of ricin A chain in deionized water and in tap water. Results were obtained within <15 min. The "Raptor" also was applied to detect bacteria of the *Enterococcus* species in Florida recreational water.[173] The method involves culturing indicator bacteria (fecal coliform bacteria and *enterococci*), ultrafiltration, and detection using the United States Environmental Protection Agency method. An aliquot of each final retentate was adsorbed on polystyrene waveguides for immunoassay with the microfluidic fiber-optic biosensor ("Raptor"). The combined ultrafiltration/biosensor procedure required 2.5 h for detection vs 24 h for the standard method.

Prostate-specific antigen (PSA), a well-established tumor marker, can be quantified in serum samples with an ultrasensitive fiber-optic biosensor.[174] PSA not only indicates prostate cancer, but also breast cancer. Serum PSA level of females are ~1 pg/mL, which is not easily detectable by conventional assays. The authors used a localized surface-plasmon coupled-fluorescence fiber-optic biosensor, combined with a sandwich immunoassay to enhance the sensitivity of conventional immunoassay. The resulting biosensor measures PSA in the range of 0.1–1000 pg/mL. Analysis of clinical samples showed good discriminate between breast cancer patients from noncancer patients. A similar configuration[175] enables the determination of alpha-fetoprotein in human serum at 0.1–100 ng/mL levels. This LOD is comparable to the conventional ELISA but the assay is less expensive, disposable, and simple to perform.

The determination of viruses in serum was accomplished with a localized surface plasmon (LSP) coupled to a fluorescence fiber-optic biosensor to diagnose the severe respiratory syndrome (SARS) caused by the coronavirus nucleocapsid protein.[176] The biosensor relies on a sandwich immunoassay combined with the LSP technique with its inherent sensitivity and can detect the nucleocapsid protein down to levels of 0.1 pg/mL, which is much better than that of the conventional immunoassay. The same group[177] also applied the method to detect swine-origin influenza A (H1N1) viruses with an LOD of 14 pg/mL. This is again more than 100-fold better than the conventional ELISA. The technique seems to have a large potential. A fiber-optic SPR immunosensor for *E. coli* bacteria has been modeled by the finite-element method.[178] The complex propagation characteristics, the formation of the coupled supermodes, and power fraction in the different regions, modal loss, differential loss, and coupling length were calculated, and the effect of the outer RI on the inner and outer surface-plasmon modes investigated with the aim to achieve the best coupling and sensitivity. The authors also show that the design of SPR fiber-optic sensors can be optimized, with respect to the maximal field penetration in the outer medium.

SPR also was used to study the kinetics of the binding of proteins to gold nanoparticles, which is slow.[179] The authors have presented a method to calculate the binding constants of protein–protein interactions in sandwich assays at ultralow concentrations using a localized SPR-coupled fluorescence fiber-optic biosensor. Specifically, the association rate constants and dissociation rate constants were determined of binding between a model antigen (total prostate-specific antigen) and its antibody. This seems to be the first time that such data have been measured at such a low concentration range in a sample as complex as human serum. Similar studies have been performed with mouse IgG and its antibody.[180,181] The same group has developed a localized surface-plasmon coupled-fluorescence fiber-optic biosensor to determine alpha-fetoprotein.[182] Fluorescently labeled antibody was conjugated to the gold nanoparticles and efficiently photoexcited by the field of the LSP. Both the sensitivity and the selectivity of the assay are much improved.

A sandwich immunoassay was performed[183–185] on the surface of a tapered optical fiber to determine interleukin-6 (IL-6) in serum. A "capture" antibody was first covalently immobilized at the fiber tip which then was dipped in serum containing fluorescently labeled anti-IL-6 antibody. A sandwich complex is formed between the capture antibody on the fiber, antigen (IL-6), and the fluorescently labeled anti-IL-6 antibody. The concentration of IL-6 is directly related to the recorded fluorescence intensity and can be detected at levels down to 5 pM (equal to 0.12 ng/mL), even in the presence of a much-higher concentration of the related protein cytokine IL-8. This reveals the high specificity and selectivity of the assay. The biosensor was successfully used to correctly determine IL-6 in two serum samples. Evanescent-wave spectroscopy was applied in a multitarget fiber-optic fluorescence immunosensor.[186] Quantum dots (QDs) were used as multicolor labels. A direct binding model assay using human IgG and its antigen demonstrated the advantages of QDs over conventional labels, and a multiplexed immunoprobe was obtained with four QD labels of different fluorescent color.

dx.doi.org/10.1021/ac303159b | *Anal. Chem.* 2013, 85, 487–508

The RI is measured in a new biosensing scheme to detect proteins.[187] A tapered fiber optic was placed in a flow cell, and transmission was measured in the NIR range at 1310 and 1550 nm, respectively. If the antibody to bovine serum albumin (anti-BSA) is placed on the tapered fiber and exposed to a solution of BSA, the latter can be detected at levels as low as 10 fg/mL. The tapered fibers have waist diameters of 5−10 μm and a total length of 1000−1200 μm. They were housed in a specially constructed holder, which served as a flow cell. The sensor is said to be selective in that 1 pg/mL of BSA can be detected in the presence of 1 pg/mL of ovalbumin. The transmission of the fiber is a function of the RI of the liquid surrounding the taper and also depends on the wavelength.

Food is another matrix where fiber-optic sensors can make assays more user-friendly. Specific target analytes include additives, bacteria, and their toxins. *Listeria monocytogenes* bacteria were detected in food with an antibody-aptamer functionalized fiber-optic biosensor.[188] Biotinylated anti-*Listeria* antibody was immobilized on a streptavidin-coated waveguide surface for capturing bacteria, and a labeled aptamer (A8) was used as the reporter. The labeled aptamer is specific for internalin A, which is an invasin protein of *L. monocytogenes*. In essence, this assay works in the sandwich format. Pathogens can be detected in pure culture and in mixture with other bacteria at a concentration of ~103 cfu per mL. The method was used to detect bacteria in artificially contaminated meat products. *Salmonella enterica* is another food-borne pathogen of worldwide concern and most commonly associated with poultry products. Valadez et al.[189] also used a sandwich structure immunoassay to develop an evanescent-wave fiber-optic biosensor for *Salmonella* in egg shell and chicken breast. An anti-*Salmonella* polyclonal antibody was immobilized on the surface of the fiber via biotin−avidin coupling. Labeled antibody served as the reporter (as a secondary antibody). The LOD of this bioprobe is ~100 cfu per mL for both pure cultures and egg and chicken breast samples after 26 h of enrichment.

PNA-Based Biosensors (DNA, Aptamers). The unique pattern of (even short) oligomers represents a powerful tool in terms of biosensing, not the least because even single mismatches of nucleobase cause large changes in the affinity between two complementary strands. An ultrasensitive system to detect DNA and its hybridization kinetics exploits evanescent-wave detection.[190] Single-stranded DNA (ssDNA) was covalently immobilized on an optical fiber via streptavidin/biotin binding, and target (i.e., complementary sequence)-DNA was labeled with fluorescent quantum dots. Hybridization results in an increased fluorescence due to the binding of target DNA with their QDs that can be "seen" by the fiber. Kinetics can also be followed by this method. Binding can be (thermally) reversed, which makes the sensor reusable up to 30 times. Leung et al.[191] reported on a label-free technique using ssDNA immobilized on a gold-coated tapered optical fiber. Hybridization of the ssDNA with its counterstrand causes the local RI to change, and this change serves as the analytical information. The system works in a flow mode and can detect target DNA in concentrations of 750 fM to 7.5 nM. Other sequences are not detected. In fact, even a single nucleotide mismatch can be distinguished. A similar approach was reported by the Lammertyn group[192] who immobilized ssDNA on gold nanoparticles and used SPR for signal readout. The same group also reported[193] on real-time monitoring of DNA hybridization and melting using a fiber-optic surface plasmon resonance (FO-SPR) sensor. Real-time monitoring of melting has rarely been studied using SPR, because most commercial instruments do not allow for dynamic and accurate temperature control above 50 °C. The FO-SPR sensor along with silica nanobead signal amplification allowed sensing inside a standard PCR thermocycler, which enabled high-resolution melting curves to be acquired. Figure 7 shows a schematic of a fiber-optic SPR DNA sensor.

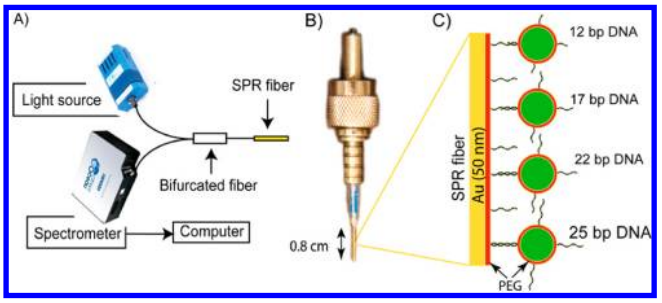

Figure 7. (Left) Schematic of the sensor with light source, fiber optics, and spectrometer. (Center) Photograph of the fiber tip with the gold coating. (Right) Schematic of the surface of the SPR fiber sensor with silica beads carrying DNA oligomers of different lengths and different numbers of base pairs. (Reproduced from ref 193, with permission of the Institute of Physics Publishing.)

Aptamers are oligomers (RNA or ssDNA) capable of selectively binding to a target analyte. They are made synthetically and usually identified by the so-called SELEX process. Sensing of Hg(II) ion via aptamers already was described in the section on ion sensors. A fiber-optic aptamer sensor for the explosive TNT[194] was obtained by immobilizing TNT on a fiber, along with its fluorescently labeled aptamer. If additional TNT is added via the sample to be analyzed, it will competitively bind to the aptamer and release it from the surface of the fiber. Fluorescence intensity will decrease as a result, because the fiber can detect fluorescence only in very close proximity. Fluorescence intensity is inversely related to the concentration of free TNT. This biosensor is highly selective and has a picomolar LOD.

Other Affinity Sensors. Various other bioaffinity interactions have been explored for purposes of sensing. Glucose again is a target of substantial interest. The state of the art in optical sensing of glucose has been reviewed by Steiner et al.[20] A fluorescence-lifetime-based fiber-optic glucose sensor was built using the glucose/galactose-binding protein (GBP) labeled with an environmentally sensitive fluorophore.[195] The protein was attached to the surface of agarose that was functionalized with nickel-nitrilotriacetic acid, or on polystyrene beads. The protein-loaded agarose or polystyrene beads were placed in a porous chamber at the end of a multimode optical fiber. If exposed to glucose, the fluorescence lifetime of the probe increased up to glucose concentrations of 100 mM. The apparent dissociation constants are 13 mM for agarose and 20 mM for polystyrene. Responses are reversible and stable, and clinical measurements were performed about every hour. This affinity sensor is biocompatible but its response is rather long. In a similar approach, the labeled GBP served as the receptor in a fiber-optic system to sense glucose in swine.[196]

Rather than using the GBP, glucose also can be sensed via competitive binding of glucose and β-cyclodextrin to concanavalin A (Con A).[197] Other than in earlier approaches, the cyclodextrin was labeled with a rhodamine, and Con A was labeled with luminescent quantum dots. Both materials were placed in a matrix of poly(ethylene glycol) and then deposited in a cavity at the distal end of an optical fiber. The binding of labeled

cyclodextrin to Con A brings the two fluorophores into close spatial proximity and enables fluorescence resonance energy transfer (FRET) to occur. Glucose binds competitively to Con A to replace the labeled cyclodextrin so that FRET will be suppressed. Animal implantation studies showed the biosensor to have good biocompatibility. Glucose was sensed with this system in the physiological concentration range (0−30 mM) over several weeks, even though Con A in earlier studies was reported not to be very stable over time. The biotin−avidin affinity system was used in a model experiment[198] involving avidin-labeled UCLNPs and biotin-labeled gold nanoparticles (Au NPs). Once the Au NPs come into proximity of the UCLNPs due to biotin/avidin affinity binding, the green emission of the UCLNPs is screened by the Au NPs, while the red emission remains unaffected. Biotinylated Au NPs were ratiometrically determined in the range of 12−250 μg/mL.

Enzymatic Biosensors. Enzymatic reactions proceed with high efficiency and specificity, and usually at temperatures below 50 °C. An SPR-based fiber-optic sensor for urea was fabricated[199] by deposition of thin layers of silver, silicon, and the enzyme urease over a length of ∼1 cm of an unclad optical fiber core. The enzyme causes the hydrolysis of urea to form ammonium and bicarbonate ions, and an increase of the local pH value. If exposed to urea, the resonance wavelength of the SPR sensor decreases with increasing concentrations of urea. The analytical range is up to 160 mM of urea, which is within its concentration in blood. Such sensors are needed, for example, during blood dialysis. Uric acid, which is another metabolite in blood and urine that often is present at elevated levels, was enzymatically detected using oxygen transduction.[200] The enzyme uricase oxidizes uric acid, and this is accompanied by the consumption of oxygen. The enzyme and an oxygen-sensitive probe were coimmobilized in a polyurethane hydrogel, and the consumption of oxygen was measured via the changes of the luminescence intensity of the probe. Uric acid can be determined in the range of 0−2 mM, and the response time is on the order of 80−100 s.

An oxygen sensor also was used as a transducer in combination with the enzyme toluene mono-oxygenase.[201] Enzymatic reaction again results in the consumption of oxygen and changes in the luminescence intensity of an oxygen-sensitive probe. The biosensor can detect toluene in wastewater with an LOD of 3 μM and a linear signal change up to 100 μM. Unfortunately, the response time is long (1 h), and the activity declines with each measurement and with storage time. Huang et al.[202] used a FOCS for oxygen as a transducer in an adrenaline biosensor. The enzyme laccase was immobilized on NPs composed of composites made from Fe_3O_4 and copper phthalocyanine. The material was deposited, along with an oxygen-sensitive membrane sensor, at the tip of an optical fiber. The enzyme catalyzes the oxidation of adrenaline under the consumption of oxygen. This is reported by the luminescent oxygen-sensing membrane. The immobilized enzyme is fairly stable, and the biosensor can sense adrenaline in 10 nM to 1 μM concentrations, with a typical response time of 30 s.

Rather than measuring the consumption of oxygen, one may also detect changes in pH values that result from enzymatic reactions. An enzymatic fiber-optic biosensor for halogenated hydrocarbons was constructed by coimmobilization of the enzyme haloalkane dehalogenase and a fluorescent pH indicator at the tip of an optical fiber.[203] This enzyme catalyzes the hydrolytic dehalogenation of halogenated aliphatic hydrocarbons. This is accompanied by a local pH change in the sensor film that can be reported using the fluorescence of the indicator. Halogenated hydrocarbons such as 1,2-dibromoethane and 3-chloro-2-(chloromethyl)-1-propene were determined in the range of 0−1.2 mM and 0−0.8 mM, respectively, with LODs of 0.133 and 0.014 mM. The sensor enables continuous and in situ monitoring of halogenated environmental pollutants. However, it is mandatory in the case of such sensors that samples are not strongly buffered and that the sample pH remains constant. The herbicide atrazine was determined via changes in local pH in a similar fashion.[204] The enzyme atrazine chlorohydrolase was immobilized on the surface of a pH-sensitive optical sensor membrane placed on a fiber-optic waveguide. Upon enzymatic dechlorination of atrazine, hydrochloric acid is released, and this is reported by the pH indicator. The response time typically is 10−20 min, and 25 ppb of atrazine is detectable. The sensor was used to determine atrazine in a soil column.

Nicotinamide adenine dinucleotide (NAD^+) is a coenzyme found in all living cells. Unlike NAD^+, reduced NAD^+ (i.e., NADH) is fluorescent with an emission peak at 460 nm if excited at 340 nm. The formation of NADH over time was exploited in fiber-optic biosensors for ethanol and formaldehyde. NAD^+ was coimmobilized with alcohol dehydrogenase on a Y-shaped optical fiber, and the production of NADH was monitored over time.[205] Ethanol was sensed in the 0.1−100 mM range with high selectivity. The system can also be applied to alcohol vapor[206] if a circulating flow cell with fresh buffer is used to refresh and wet the enzyme on the fiber. The biosensor is useful for the continuous monitoring of 0.3−300 ppm of alcohol (for example, in breath analysis). Similarly, the coimmobilization of NAD^+ and the enzyme formaldehyde dehydrogenase on an optical fiber gave a biosensor for gaseous formaldehyde[207,208] by measuring the fluorescence of the NADH formed in the enzymatic reaction. The system utilizes an ultraviolet-light-emitting diode with a peak emission at 335 nm as the light source for the photoexcitation of NADH. Again, a circulating buffer was used to retain the activity of the enzyme. The analytical range is from 2.5 ppb to 10 ppm, and the LOD is 0.75 ppb.

Whole Cell Sensors. Whole cells are excellent indicators for a variety of parameters, in particular for toxic compounds. Unless genetically trimmed to a specific analyte (such as a certain metal ion), they respond unspecifically and thus represent an excellent means for monitoring toxicity and pollutants. A fiber-optic biosensor for monitoring air toxicity[209] is making use of bioluminescent bacteria immobilized in an alginate matrix on the bottom of the wells in a 96-well microplate. If exposed to toxic compounds present in air, bioluminescence is suppressed. Chloroform can be detected by this method at levels as low as 6.6 ppb. This system was then adapted to a portable fiber-optic biosensor. The same group[210] immobilized two other bacterial strains with the aim to develop a flow-through fiber-optic sensing system for online monitoring of toxic pollutants in water. The sensor was successfully tested for its ability to detect pollutants in flowing tap water and surface water over 24 h, but a loss of functionality of the bacteria was observed after longer periods. The use of whole cells for fiber-optic sensing has been reviewed by this group.[211]

Bacteria out of the coliform subgroup possess a high activity of the enzyme asparaginase. They were coimmobilized with the indicator Phenol Red in a sol−gel film to construct a miniaturized fiber-optic biosensor for monitoring L-asparagine.[212] The enzyme hydrolyzes L-asparagine to form L-aspartic acid and ammonia, and the associated increase in local pH results in a change of the absorption spectrum of the pH indicator. The biosensor has a wide operational range (0.1 M to 1 nM), and L-asparagine was

dx.doi.org/10.1021/ac303159b | Anal. Chem. 2013, 85, 487−508

determined with an LOD of 1 nM. The biosensor only needs 5 μL of a sample per assay. The biosensor is stable for 40 days if stored at 4 °C and was applied to quantify L-asparagine in mango juice, pineapple juice, wine, and tea. Microalgae are another living species that were applied to biosensing. Encapsulated in a silicate sol−gel matrix, they were found to respond to herbicides, such as simazine, atrazine, propazine, and linuron,[213] in giving an increase of chlorophyll fluorescence, because the herbicides destroy photosystem II. The biosensor works over a wide range of herbicide concentrations (from 0.5 μg/mL to 10 mg/L) but LODs at ∼0.1 μg/mL are desirable. The response is partially reversible, and the weed killer 2,4-dichlorophenoxy acetic acid (2,4-D) does not interfere.

■ ADVANCED OPTICAL SENSING SCHEMES AND MATERIALS

This section covers two aspects (new spectroscopies and new materials), because they often come together. SPR remains to be a spectroscopic method of substantial activity, not the least because it is a label-free technique and can be coupled to fiber-optic sensing in many ways. Some examples for respective sensors have been presented in earlier section. In addition, the known fact that a nanometer-thin overlayer on the basic (gold) layer of SPR sensors can help to improve their sensitivity recently was theoretically underpinned in a simulation based on the theory of attenuated total internal reflection.[214] The authors simulated a metallic layer covered with silicon and an oxide layer. The thickness of the metal layer can be optimized to achieve the most pronounced dip at the resonance condition and to improve sensitivity. Similarly, the properties of a SPR-based fiber-optic sensor for gas sensing in the visible range and using a nanocomposite coating were simulated.[215] It was found that among the nanoparticles (silver, gold, or indium tin oxide (ITO)) added to the host dielectric matrix (WO_3, SnO_2, and TiO_2), the sensor with the ITO-doped TiO_2 coating possesses the best sensitivity. Star-shaped Au NPs were used to modify the surface in a fiber-optic localized SPR sensor.[216] Localized SPR was induced by the particles that were self-assembled on the surface of a tapered optical fiber, and transmission spectra were acquired at different concentrations of ethanol and of solutions of a blue dye. The transmission spectra show that the Au NPs are sensitive to the dielectric properties of the surrounding medium. Multiple particle-based plasmon resonances was exploited in a multiplexed fiber-optic affinity sensor,[217] using antidinitrophenyl antibody and streptavidin, respectively. Multiple resonances were achieved by chemical immobilization of silver nanoparticles (Ag NPs) and gold nanorods on two uncladded portions of an optical fiber. Differences in the morphology and nature of the two materials were exploited to yield multiple plasmonic absorptions at 405 and 780 nm in the absorption spectrum. This enabled real-time and simultaneous detection of multiple analyte-probe pairs if the particles carry respective receptors.

Transient and traveling LPGs have been reported that are capable of detecting nanometer variations in the thickness of a fiber coating.[218] The sensing platform is based on a transient and traveling LPG in a single-mode optical fiber. The LPG is generated by pulsed acoustic waves that propagate along the fiber. While demonstrated for (distributed) measurement of temperature along a fiber, it is reasonable to assume that chemical and biochemical sensing also can be accomplished by coating the fiber with ultrathin multilayers that respond to (bio)chemical analytes.

A portable biochemical reflectometric detector based on fiber-optic sensors was introduced.[219] It was used to determine hemoglobin and an enzyme (alanine aminotransferase). A light-emitting diode serves as the light source and was coupled to the Y-shaped fiber optic to detect the reflected signal and to monitor the status of the system at the same time. The results were compared with those obtained with large instruments, and the correlation coefficient was found to be 0.981. The device has good accuracy, fast response, and is said to be useful in situations such as field blood testing and in function tests for athletes. Commodity instruments such as mobile phones, computer screens, flatbed scanners, and digital cameras are finding more and more uses in sensing schemes and will replace sophisticated (and expensive) scientific instrumentation in some cases. It has been shown, for example, that oxygen can be sensed and imaged using a respective sensor film and a commercial digital camera.[220] A specially designed fluorescent sensor film containing a quenchable red-emitting probe for oxygen along with a green-emitting reference fluorophore was photographed. The camera acts as a rudimentary spectrometer for ratiometric imaging, with one excitation wavelength (using a blue LED) and multiple (three-wavelength) readout in the red, green, and blue (RGB) part of the visible spectrum. The ratio of the (oxygen-dependent) intensity of the red channel and that of the inert green intensity represents a stable signal that can be related to oxygen particle pressure. In fact, even two parameters (oxygen and pH value) may be sensed simultaneously and in vivo (in wounds) by acquiring one image.[221] An LED array placed in front of the camera is used for photoexcitation. Three dyes, with emission peaks that match the RGB channels of the camera, were chosen to create a sensor film. Oxygen is detected at 650 nm (signal stored in the red channel), pH at 530 nm (signal stored in the green channel), and the signal of the reference fluorophore at 440 nm (stored in the blue channel).

Sensing schemes based on evanescent-wave absorption or attenuated total reflection remain attractive tools. They can be applied to sense the RI of a solution, the thickness and RI of (bio)chemical coatings, and the UV, visible, or IR absorption of the analyte close to the core/solution interface. Attenuated total reflection is particularly powerful when monitoring the absorption of species in turbid media. A respective fiber-optic sensor was applied[222] to study the bulk absorption and evanescent wave absorbance of micrometer-sized graphite flakes and spherical glassy carbon suspensions. The technique is superior to bulk absorptiometry due to high scattering of the particles. The evanescent-wave absorbance using a coiled fiber-optic sensor, in contrast, is insensitive to scattering of suspended particles, especially for suspensions of graphite flakes. The RI of a solution is affected by numerous parameters and chemical species, but respective sensors can be applied to rather specific situations and are usually quite robust. A simple fiber-optic RI sensor based on tapered fiber was demonstrated[223] to detect methanol, ethanol, 1-propanol, and 2-propanol. The change of the RI in the evanescent field in the tapering region of the fiber changes the output power of the transmitted light. The optimum radius of the tapered fiber core was calculated (∼282 μm), and the output intensity increases slowly as the fraction of the alcohols increases from 10% to 50%. However, the intensity increases drastically as the methanol fraction approaches 100%, which limits the wider applicability of this sensor.

Evanescent-wave absorbance-based fiber-optic sensing of *E. coli* at 280 nm was demonstrated.[224] The technique is label-free and exploits the changes in absorbance by cells on the surface

dx.doi.org/10.1021/ac303159b | *Anal. Chem.* 2013, 85, 487−508

of a U-shaped optical fiber. Bending a decladded fiber into a U-shaped structure enhances the penetration depth of evanescent waves and, hence, the sensitivity of the probe. The portable optical setup consists of a 280-nm LED, a spectrometer, and a U-bent fiber-optic probe with a core diameter of 200 μm, a 0.75-mm bend radius, and an effective probe length of 1 cm and can detect <1000 cfu/mL of *E. coli*. However, the probe works far in the UV, where many other species cause absorption, and it will be selective only if appropriate antibodies are being applied. An integrated fiber-optic sensor was reported[225] that uses incoherent broadband cavity-enhanced absorption spectroscopy for the detection of NIR absorbing dyes in nanoliter volumes. Absorption was measured in a 100-μm gap between the ends of two short segments of multimode graded-index fiber that were integrated into a capillary to form a 9.5-cm optical resonator. It was concluded that the minimum detectable absorption change is 1.6×10^{-5} if pressure can be kept constant.

A current trend in optical sensing generally is to identify new (nano)materials that can improve the performance (i.e., mainly the LOD and selectivity) of existing sensors. For example, a silver-embedded zeolite thin film enables improved in situ and real-time fiber-optic monitoring of Hg^{2+} ions, in terms of sensitivity and selectivity.[143] The intensity of the reflection by the zeolite-coated fiber changes monotonically with the variation of the concentration of Hg^{2+} ions. Similarly, the addition of nanocrystalline TiO_2 to the cladding of an optical fiber sensor improves the signal-to-noise ratio of a FOCS for ammonia and enables the gas to be sensed in the 50−500 ppm concentration range.[226] The TiO_2 acts as a sensing material, and the spectral characteristics of the sensor were studied. However, the sensor is not selective in also responding to vapors of methanol and ethanol. The implementation of zinc oxide waveguiding nanowires can enlarge the surface and enhance sensitivity. This is of particular significance in the case of microsystems with flow-through cells that had rather small optical path lengths.

The addition of (scattering) microparticles is known to strongly enhance the signal and, thus, the performance of fluorescence lifetime-based optical sensors. Chatni et al.[227] have compared TiO_2 microparticles and nanoparticles, and $BaSO_4$, chromium, CuO, diamond, gold, PbO, and ZnS microparticles and found that 2-μm-sized particles amplify fluorescence much better than any NPs. Materials with high RIs perform better, provided they have low absorbance in the visible range. The results allowed sensor membranes to be optimized, as shown for the case of a porphyrin-based oxygen optrode. The fluorescence enhancement effect caused by metallic nanoparticles was studied using the scattering theory of evanescent waves by a metallic nanoparticle.[228] The nanoparticles not only provide strong local field to enhance the fluorescence signal of fluorophores, but also help to scatter the fluorescence signal and to increase the far-field detectable signals. The effects of the radius of Au NPs, the fluorophore−particle separation, and fiber−particle separation on the fluorescence enhancement were discussed. Microbeads with pH sensing capability were placed in a micro flow-through fluorometer and used for determination of pH values inside microfluidic segments.[229] In contrast to dissolved indicator dyes, the response of the sensor particles is not interfered by the surrounding solution. The typical change of pH during cell cultivation can be used to monitor the kinetics of cell cultivation inside single volumes in the nanoliter range, so that information about the metabolic activity of the organism can be obtained. Microparticulate matter also was applied[230] in a dual-indicator-based sensor material for simultaneous sensing of air pressure (via oxygen partial pressure) and temperature in order to suppress fluorescence resonance energy transfer between the fluorescent probes.

Photonic crystals (PhCs) represent a fairly new but unexplored class of sensor materials. PhCs were combined with fiber-based absorption spectroscopy,[231] and it was observed that highly sensitive evanescent field absorption occurs when using an optimized structure of PhC fibers with defected core. This structure results in twice the sensitivity of a commercial spectrophotometer, which suggests its use when handling minute samples such as those common in microchip technology. Recently, multiparameter sensing based on photonic *liquid crystal* fibers was demonstrated for the first time.[232] While applied to sensing temperature, electrical field, and hydrostatic pressure in this work, the method is likely also to work in chemical sensing if proper recognition chemistries are identified. PhCs have been applied in sensors for pH,[233,234] humidity,[235,236] and others, and their responses to (bio)chemical analytes has been reviewed.[237] Figure 8 shows the color changes of such a sensor layer as a function of the pH value of the material with which it is in contact. PhC-based sensors have the unique advantage of not requiring molecular indicator probes and allow bare-eye readouts, because of their distinct color changes.

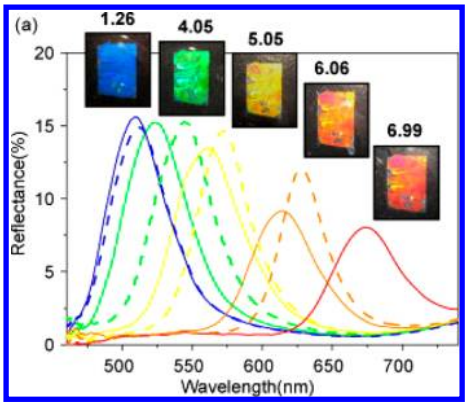

Figure 8. Visual color change and respective reflectance spectra of a hydrogel pH sensor containing a photonic crystal structure. pH values extend from pH 1.26 to pH 6.99, as indicated. The solid-curve spectra are those obtained after an increase in pH, while the dashed curves are those obtained after the pH value has been lowered. (Reproduced from ref 234, with permission of Elsevier.)

An air-suspended solid-core PhC fiber sensor was constructed that enables quantitative broadband evanescent-field sensing of holes in the cladding of the waveguide.[238] The fraction of light entering the hollow cladding can be tuned via the core diameter of the fiber. Dispersion measurements are in excellent agreement with theory, and the zero dispersion wavelength can be tuned via the core diameter. Design parameters for absorption sensors are discussed, and it was concluded that an increase in sensitivity by 3 orders of magnitude may be feasible, compared to standard cuvette measurements. The principal applicability of the approach was demonstrated by acquiring the absorption spectrum of a (green) solution of nickel chloride. It was found to be in excellent agreement with the reference spectrum, even though the sample volume was 3 orders of magnitude smaller.

AUTHOR INFORMATION

Corresponding Author

*Tel.: +49 941 943 4065 (X.-D.W.), +49 941 943 4058 (O.S.W.). Fax: +49 941 943 4064 (X.-D.W.). E-mail: xmuwxd@gmail.com (X.-D.W.), Otto.Wolfbeis@ur.de (O.S.W.).

Notes

The authors declare no competing financial interest.

Biographies

Xu-dong Wang, born in 1985, received his Ph.D. degree in Chemistry from Xiamen University (Xiamen, China) in 2011. Since then, he has worked as a postdoctoral fellow in the group of Prof. Otto S. Wolfbeis at the University of Regensburg within an Alexander von Humboldt fellowship. His research interests are in the design of optical chemical and biosensors, nanosensors and molecular probes, developing novel (bio)sensing schemes, (nano)-materials and methods, and their applications to biological and chemical analysis. He has authored or coauthored more than 20 articles over the past five years, and his current h-index is 10 (Dec. 2012).

Otto S. Wolfbeis was a Full Professor of Analytical and Interface Chemistry at the University of Regensburg, Germany, from 1995 to 2012. He has authored numerous papers and reviews on optical (fiber) chemical sensors, fluorescent probes, labels and bioassays, on advanced (nano)-materials for use in sensing schemes, and in spectroscopic methods including fluorescence (lifetime) imaging. He has (co)edited several books, and has acted as the (co)organizer of several conferences related to fluorescence spectroscopy (*MAF*) and to chemical sensors and biosensors (*Europtrode*). His h-index is 68 (Dec. 2012). He is one of the 10 curators of *Angewandte Chemie*, the Editor-in-Chief of *Microchimica Acta*, and one of the three editors of *Methods and Applications in Fluorescence*. (Also see: www.wolfbeis.de.)

ACKNOWLEDGMENTS

X.-D.W. thanks the Alexander von Humboldt Foundation (Bonn) for a fellowship.

REFERENCES

(1) Wolfbels, O. S. *Anal. Chem.* **2008**, *80*, 4269.
(2) McDonagh, C.; Burke, C. S.; MacCraith, B. D. *Chem. Rev.* **2008**, *108*, 400.
(3) Guo, Z.; Song, N. R.; Moon, J. H.; Kim, M.; Jun, E. J.; Choi, J.; Lee, J. Y.; Bielawski, C. W.; Sessler, J. L.; Yoon, J. *J. Am. Chem. Soc.* **2012**, *134* (43), 17846−17849 (DOI: 10.1021/ja306891c).
(4) Udd, E.; Spillman, W. B., Jr. *Fiber Optic Sensors*, 2nd Edition; Wiley & Sons: New York, 2011.
(5) Nagl, S.; Wolfbeis, O. S. In *Springer Series on Fluorescence: Standardization and Quality Assurance in Fluorescence Measurements I*; Resch-Genger, U., Ed.; Springer: Berlin, Heidelberg: 2008; Vol. 5, p 325.
(6) Sun, K.; Wu, N.; Guthy, C.; Wang, X. In *Advances in Nanomaterials and Nanostructures*; Ceramic Transactions 229; American Ceramic Society: Westerville, OH, 2011; p 163.
(7) Wolfbeis, O. S. *Adv. Mater.* **2008**, *20*, 3759.
(8) Wolfbeis, O. S. *Adv. Mat.* **2008**, *20*, 3759.
(9) Tao, S.; Guo, H. In *Chemical Sensors: Properties, Performance and Applications*; Harrison, R. V., Ed.; Nova Science Publishers, Inc.: New York, 2011; p 63.
(10) Duffin, K.; Johnstone, W.; McGettrick, A.; Moodie, D.; Stewart, G.; Thursby, G.; Culshaw, B. *Curr. Anal. Chem.* **2008**, *4*, 391.
(11) Aernecke, M. J.; Walt, D. R. In *Nano and Microsensors for Chemical and Biological Terrorism Surveillance*; Tok, J. B.-H., Ed.; The Royal Society of Chemistry: London, 2008; p 98.
(12) Stich, M. I. J.; Fischer, L. H.; Wolfbeis, O. S. *Chem. Soc. Rev.* **2010**, *39*, 3102.
(13) Kocincova, A. S.; Borisov, S. M.; Krause, C.; Wolfbeis, O. S. *Anal. Chem.* **2007**, *79*, 8486.
(14) Valledor, M.; Campo, J. C.; Ferrero, F.; Sánchez-Barragán, I.; Costa-Fernández, J. M.; Sanz-Medel, A. *Sens. Actuators B* **2009**, *139*, 237.
(15) Mayr, T.; Borisov, S. M.; Abel, T.; Enko, B.; Waich, K.; Mistlberger, G. n.; Klimant, I. *Anal. Chem.* **2009**, *81*, 6541.
(16) Ligler, F. S.; Taitt, C. R. *Optical Biosensors: Today and Tomorrow*; Elsevier Science: Amsterdam, 2008.
(17) Borisov, S. M.; Wolfbeis, O. S. *Chem. Rev.* **2008**, *108*, 423.
(18) Orellana, G.; Haigh, D. *Curr. Anal. Chem.* **2008**, *4*, 273.
(19) Yeo, T. L.; Sun, T.; Grattan, K. T. V. *Sens. Actuators A* **2008**, *144*, 280.
(20) Steiner, M.-S.; Duerkop, A.; Wolfbeis, O. S. *Chem. Soc. Rev.* **2011**, *40*, 4805.
(21) Achatz, D.; Ali, R.; Wolfbeis, O. S. In *Topics in Current Chemistry*, Vol. *300*; Prodi, L., Montalti, M., Zaccheroni, N., Eds.; Springer: Berlin/Heidelberg, 2011; p 29.
(22) Sun, L.-N.; Peng, H.; Stich, M. I. J.; Achatz, D.; Wolfbeis, O. S. *Chem. Commun.* **2009**, 5000.
(23) Monzón-Hernández, D.; Luna-Moreno, D.; Martinez-Escobar, D. *Sens. Actuators B* **2009**, *136*, 562.
(24) Silva, S. F.; Coelho, L.; Frazao, O.; Santos, J. L.; Malcata, F. X. *IEEE Sens. J.* **2012**, *12*, 93.
(25) Javahiraly, N.; Perrotton, C.; Slaman, M.; Dam, B.; Meyrueis, P. *Proc. SPIE, Int. Soc. Opt. Eng.* **2012**, *8368*, 836804.
(26) Perrotton, C.; Javahiraly, N.; Slaman, M.; Dam, B.; Meyrueis, P. *Opt. Express* **2011**, *19*, A1175.
(27) Bhatia, P.; Gupta, B. D. *Proc. SPIE, Int. Soc. Opt. Eng.* **2012**, *8351*, 83511V.
(28) Matsuyama, N.; Okazaki, S.; Nakagawa, H.; Sone, H.; Fukuda, K. *Thin Solid Films* **2009**, *517*, 4650.
(29) Watanabe, T.; Okazaki, S.; Nakagawa, H.; Murata, K.; Fukuda, K. *Sens. Actuators B* **2010**, *145*, 781.
(30) Yang, M. H.; Yang, Z.; Dai, J. X.; Zhang, D. S. *Sens. Actuators, B* **2012**, *166*, 632.
(31) Wang, D. Y.; Wang, Y. M.; Gong, J. M.; Wang, A. B. *IEEE Photonics Technol. Lett.* **2011**, *23*, 733.
(32) Okazaki, S.; Nakagawa, H.; Murata, K.; Fukuda, K. *Sens. Lett.* **2011**, *9*, 688.
(33) Wei, X.; Wei, T.; Xiao, H.; Lin, Y. S. *Sens. Actuators, B* **2008**, *134*, 687.
(34) Tang, X. L.; Remmel, K.; Lan, X. W.; Deng, J. D.; Xiao, H.; Dong, J. H. *Anal. Chem.* **2009**, *81*, 7844.
(35) Grobnic, D.; Mihailov, S. J.; Walker, R. B.; Cuglietta, G.; Smelser, C. W. *Proc. SPIE, Int. Soc. Opt. Eng.* **2011**, *7753*, 77537D.
(36) Khotiaintsev, S.; Svyryd, V.; del Puerto, H. B. M. *Sens. Mater.* **2009**, *21*, 13.
(37) Wang, H.; Wang, Q.; Chang, J.; Zhang, X.; Zhang, S.; Ni, J. *Laser Phys.* **2008**, *18*, 491.
(38) Wu, X.; Wang, Y.; Chen, L.; Huang, X. *Proc. SPIE, Int. Soc. Opt. Eng.* **2008**, *6830*, 68301B/1.
(39) Wu, X. J.; Wang, P.; Wang, Z. B.; Li, X.; Tian, E. M. *Spectrosc. Spectral Anal. (Beijing, China)* **2009**, *29*, 2365.
(40) Cubillas, A. M.; Lazaro, J. M.; Conde, O. M.; Petrovich, M. N.; Lopez-Higuera, J. M. *Sensors* **2009**, *9*, 6261.
(41) Cubillas, A. M.; Lazaro, J. M.; Conde, O. M.; Petrovich, M. N.; Lopez-Higuera, J. M. *Sensors* **2009**, *9*, 490.
(42) Yu, K. L.; Wu, C. Q.; Wang, Z. *IEEE Sens. J.* **2010**, *10*, 728.
(43) Fei, Y.; Li, Q.; Bing, Q. *J. Lightwave Technol.* **2009**, *27*, 5356.
(44) Verma, R. K.; Gupta, B. D. *J. Opt. Soc. Am. A* **2010**, *27*, 846.
(45) Grosch, A.; Beushausen, V.; Wackerbarth, H.; Thiele, O.; Berg, T.; Grzeszik, R. *J. Quant. Spectrosc. Radiat. Transfer* **2011**, *112*, 994.
(46) Wang, X.-D.; Chen, H.-X.; Zhao, Y.; Chen, X.; Wang, X.-R.; Chen, X. *TrAC, Trends Anal. Chem.* **2010**, *29*, 319.
(47) Koshiba, Y.; Nakamura, Y.; Ito, D.; Yokoyama, T.; Okazaki, S.; Nakagawa, H.; Arai, T. *Talanta* **2010**, *82*, 1495.
(48) Panahi, A. *Proc. SPIE, Int. Soc. Opt. Eng.* **2009**, *7314*, 73140D.
(49) Nakamura, Y.; Ito, D.; Yokoyama, T.; Okazaki, S.; Nakagawa, H.; Arai, T. *Sens. Lett.* **2008**, *6*, 951.
(50) Guillaume, F.; Greden, K.; Smyrl, W. H. *J. Electrochem. Soc.* **2008**, *155*, J213.

(51) Riss, H. W.; Meyer, E. I.; Niepagenkemper, O. *Limnol. Oceanogr.* **2008**, *6*, 200.
(52) Mishra, A.; Starly, B. *Microfluid. Nanofluid.* **2009**, *6*, 373.
(53) Heller, A.; Fischer, L. H.; Wolfbeis, O. S.; Goepferich, A. *Exp. Cell Res.* **2012**, *318*, 1667.
(54) Kocincová, A. S.; Nagl, S.; Arain, S.; Krause, C.; Borisov, S. M.; Arnold, M.; Wolfbeis, O. S. *Biotechnol. Bioeng.* **2008**, *100*, 430.
(55) Bagshaw, E. A.; Wadham, J. L.; Mowlem, M.; Tranter, M.; Eveness, J.; Fountain, A. G.; Telling, J. *Environ. Sci. Technol.* **2011**, *45*, 700.
(56) Xiong, Y.; Xu, J.; Zhu, D. Q.; Duan, C. F.; Guan, Y. F. *J. Sol–Gel Sci. Technol.* **2010**, *53*, 441.
(57) Xiong, Y.; Xu, J.; Wang, J. W.; Guan, Y. F. *Anal. Bioanal. Chem.* **2009**, *394*, 919.
(58) Xiong, Y.; Zhu, D. Q.; Chen, S. H.; Peng, H.; Guan, Y. F. *J. Fluoresc.* **2010**, *20*, 269.
(59) Chen, R.; Farmery, A. D.; Chen, R.; Hahn, C. E. W. *Proc. SPIE, Int. Soc. Opt. Eng.* **2011**, *8199*, 819902.
(60) Chen, R. S.; Farmery, A. D.; Obeid, A.; Hahn, C. E. W. *IEEE Sens. J.* **2012**, *12*, 71.
(61) Chipman, L.; Huettel, M.; Berg, P.; Meyer, V.; Klimant, I.; Glud, R.; Wenzhoefer, F. *Limnol. Oceanogr.* **2012**, *10*, 304.
(62) Ganesh, A. B.; Radhakrishnan, T. K. *Opt. Lasers Eng.* **2008**, *46*, 321.
(63) Mistlberger, G. n.; Koren, K.; Borisov, S. M.; Klimant, I. *Anal. Chem.* **2010**, *82*, 2124.
(64) Stich, M. I. J.; Schaeferling, M.; Wolfbeis, O. S. *Adv. Mater.* **2009**, *21*, 2216.
(65) Lo, Y. L.; Chu, C. S.; Yur, J. P.; Chang, Y. C. *Sens. Actuators, B* **2008**, *131*, 479.
(66) Fischer, L. H.; Stich, M. I. J.; Wolfbeis, O. S.; Tian, N.; Holder, E.; Schäferling, M. *Chem.—Eur. J.* **2009**, *15*, 10857.
(67) Borisov, S.; Klimant, I. *Microchim. Acta* **2009**, *164*, 7.
(68) Fischer, L. H.; Borisov, S. M.; Schaeferling, M.; Klimant, I.; Wolfbeis, O. S. *Analyst* **2010**, *135*, 1224.
(69) Chu, C. S.; Lo, Y. L. *Sens. Actuators, B* **2008**, *134*, 711.
(70) Borisov, S. M.; Nuss, G.; Haas, W.; Saf, R.; Schmuck, M.; Klimant, I. *J. Photochem. Photobiol. A* **2009**, *201*, 128.
(71) Borisov, S. M.; Papkovsky, D. B.; Ponomarev, G. V.; DeToma, A. S.; Saf, R.; Klimant, I. *J. Photochem. Photobiol. A* **2009**, *206*, 87.
(72) Mak, C. S. K.; Pentlehner, D.; Stich, M.; Wolfbeis, O. S.; Chan, W. K.; Yersin, H. *Chem. Mater.* **2009**, *21*, 2173.
(73) Achatz, D. E.; Meier, R. J.; Fischer, L. H.; Wolfbeis, O. S. *Angew. Chem., Int. Ed.* **2011**, *50*, 260.
(74) Tiwari, V. S.; Luanje, A. T.; Kalluru, R. R.; Yueh, F. Y.; Singh, J. P. *Rev. Sci. Instrum.* **2011**, *82*.
(75) Jarzebinska, R.; Korposh, S.; James, S.; Batty, W.; Tatam, R.; Lee, S.-W. *Anal. Lett.* **2012**, *45*, 1297.
(76) Korposh, S.; Selyanchyn, R.; Yasukochi, W.; Lee, S. W.; James, S. W.; Tatam, R. P. *Mater. Chem. Phys.* **2012**, *133*, 784.
(77) Kharat, H. J.; Kakde, K. P.; Savale, P. A.; Datta, K.; Ghosh, P.; Shirsat, M. D. *Optoelectron. Adv. Mater.–Rapid Commun.* **2008**, *2*, 553.
(78) Korposh, S. O.; Sharkan, Y. P.; Ramsden, J. J. *Sens. Actuators, B* **2008**, *129*, 473.
(79) Tao, S. Q.; Fanguy, J. C.; Sarma, T. V. S. *IEEE Sens. J.* **2008**, *8*, 2000.
(80) Renganathan, B.; Sastikumar, D.; Gobi, G.; Yogamalar, N. R.; Bose, A. C. *Opt. Laser Technol.* **2011**, *43*, 1398.
(81) Renganathan, B.; Sastikumar, D.; Gobi, G.; Yogamalar, N. R.; Bose, A. C. *Sens. Actuators, B* **2011**, *156*, 263.
(82) Jalal, A. H.; Yu, J. S.; Nnanna, A. G. A. *Appl. Opt.* **2012**, *51*, 3768.
(83) Schmitt, K.; Rist, J.; Peter, C.; Wollenstein, J. *Microsyst. Technol.* **2012**, *18*, 843.
(84) Peng, L. R.; Yang, X. H.; Yuan, L. B.; Wang, L. L.; Zhao, E. M.; Tian, F. J.; Liu, Y. X. *Opt. Commun.* **2011**, *284*, 4810.
(85) Mader, H. S.; Wolfbeis, O. S. *Anal. Chem.* **2010**, *82*, 5002.
(86) Ali, R.; Saleh, S. M.; Meier, R. J.; Azab, H. A.; Abdelgawad, I. I.; Wolfbeis, O. S. *Sens. Actuators, B* **2010**, *150*, 126.
(87) Chu, C. S.; Lo, Y. L. *Sens. Actuators, B* **2009**, *143*, 205.
(88) Chu, C. S.; Lo, Y. L. *Sens. Actuators, B* **2008**, *129*, 120.
(89) Dansby-Sparks, R. N.; Jin, J.; Mechery, S. J.; Sampathkumaran, U.; Owen, T. W.; Yu, B. D.; Goswami, K.; Hong, K. L.; Grant, J.; Xue, Z. L. *Anal. Chem.* **2010**, *82*, 593.
(90) Ali, R.; Lang, T.; Saleh, S. M.; Meier, R. J.; Wolfbeis, O. S. *Anal. Chem.* **2011**, *83*, 2846.
(91) Orghici, R.; Willer, U.; Gierszewska, M.; Waldvogel, S. R.; Schade, W. *Appl. Phys. B–Lasers Opt.* **2008**, *90*, 355.
(92) Börner, S.; Orghici, R.; Waldvogel, S. R.; Willer, U.; Schade, W. *Appl. Opt.* **2009**, *48*, B183.
(93) Ohira, S. I.; Dasgupta, P. K.; Schug, K. A. *Anal. Chem.* **2009**, *81*, 4183.
(94) Ohira, S. I.; Wanigasekar, E.; Rudkevich, D. M.; Dasgupta, P. K. *Talanta* **2009**, *77*, 1814.
(95) Ding, L.; Huang, L.; Huang, J.; Zhong, Y.; Fan, D. *Proc. SPIE, Int. Soc. Opt. Eng.* **2010**, *7673*, 76730Z.
(96) Dooly, G.; Fitzpatrick, C.; Lewis, E. *Sens. Actuators, B* **2008**, *134*, 317.
(97) Qin, H.; Kulkarni, A.; Zhang, H.; Kim, H.; Jiang, D.; Kim, T. *Sens. Actuators, B* **2011**, *158*, 223.
(98) Bezunartea, M.; Estella, J.; Echeverría, J. C.; Elosúa, C.; Bariáin, C.; Laguna, M.; Luquin, A.; Garrido, J. J. *Sens. Actuators, B* **2008**, *134*, 966.
(99) Elosua, C.; Bariain, C.; Matias, I. R.; Arregui, F. J.; Luquin, A.; Vergara, E.; Laguna, M. *Sens. Actuators, B* **2008**, *130*, 158.
(100) Aguirre, S. M.; Hipatl, C. M.; Mixcóatl, J. C.; Pérez, G. B.; Merino, R. P. *AIP Conf. Proc.* **2008**, *992* (RIAO/OPTILAS 2007), 969.
(101) Mariammal, R. N.; Ramachandran, K.; Renganathan, B.; Sastikumar, D. *Sens. Actuators, B* **2012**, *169*, 199.
(102) Mariammal, R. N.; Susila, V. M.; Renganathan, B.; Sastikumar, D.; Ramachandran, K. *Sens. Lett.* **2012**, *10*, 18.
(103) Manivannan, S.; Saranya, A. M.; Renganathan, B.; Sastikumar, D.; Gobi, G.; Park, K. C. *Sens. Actuators, B* **2012**, *171–172*, 634.
(104) Cusano, A.; Consales, M.; Crescitelli, A.; Penza, M.; Aversa, P.; Veneri, C. D.; Giordano, M. *Carbon* **2009**, *47*, 782.
(105) Zhang, H.; Kulkarni, A.; Kim, H.; Woo, D.; Kim, Y. J.; Hong, B. H.; Choi, J. B.; Kim, T. *J. Nanosci. Nanotechnol.* **2011**, *11*, 5939.
(106) Kumeria, T.; Parkinson, L.; Losic, D. *Nanoscale Res. Lett.* **2011**, *6*.
(107) Kittidechachan, M.; Sripichai, I.; Supakum, W.; Thuamthai, S.; Angkaew, S.; Limsuwan, P. *Adv. Mater. Res.* **2008**, *55*, 509.
(108) Khomenko, A. V.; Tapia-Mercado, J.; Garcia-Zarate, M. A. *Rev. Mex. Fis.* **2010**, *56*, 208.
(109) Chen, L. H.; Li, T.; Chan, C. C.; Menon, R.; Balamurali, P.; Shaillender, M.; Neu, B.; Ang, X. M.; Zu, P.; Wong, W. C.; Leong, K. C. *Sens. Actuators, B* **2012**, *169*, 167.
(110) Shukla, S. K.; Tiwari, A.; Parashar, G. K.; Mishra, A. P.; Dubey, G. C. *Talanta* **2009**, *80*, 565.
(111) Consales, M.; Buosciolo, A.; Cutolo, A.; Breglio, G.; Irace, A.; Buontempo, S.; Petagna, P.; Giordano, M.; Cusano, A. *Sens. Actuators, B* **2011**, *159*, 66.
(112) Akita, S.; Sasaki, H.; Watanabe, K.; Seki, A. *Sens. Actuators, B* **2010**, *147*, 385.
(113) Viegas, D.; Goicoechea, J.; Corres, J. M.; Santos, J. L.; Ferreira, L. A.; Araujo, F. M.; Matias, I. R. *Meas. Sci. Technol.* **2009**, *20*.
(114) Estella, J.; de Vicente, P.; Echeverria, J. C.; Garrido, J. J. *Sens. Actuators, B* **2010**, *149*, 122.
(115) Zhao, Z. J.; Duan, Y. X. *Sens. Actuators, B* **2011**, *160*, 1340.
(116) Løkken, T. V. *J. Nat. Gas Sci. Eng.* **2012**, *7*, 7.
(117) Srivastava, S. K.; Verma, R.; Gupta, B. D. *Sens. Actuators, B* **2011**, *153*, 194.
(118) Xiong, F. B.; Sisler, D. *Opt. Commun.* **2010**, *283*, 1326.
(119) Hu, X.; Tao, S. *IEEE Sens. J.* **2011**, *11*, 2032.
(120) Andrawis, A.; Ranjitkar, B.; Yan, X.; Peng, Y. *Proc. SPIE, Int. Soc. Opt. Eng.* **2010**, *7673*, 76730P.
(121) Richter, A.; Paschew, G.; Klatt, S.; Lienig, J.; Arndt, K.-F.; Adler, H.-J. *Sensors* **2008**, *8*, 561.
(122) Gu, B.; Yin, M. J.; Zhang, A. P.; Qian, J. W.; He, S. L. *Opt. Express* **2009**, *17*, 22296.

(123) Yin, M. J.; Gu, B. B.; Zhao, Q. A.; Qian, J. W.; Zhang, A.; An, Q. F.; He, S. L. *Anal. Bioanal. Chem.* **2011**, *399*, 3623.
(124) Gui, Z. L.; Qian, J. W.; Yin, M. J.; An, Q. F.; Gu, B. B.; Zhang, A. *J. Mater. Chem.* **2010**, *20*, 7754.
(125) Gu, B. B.; Yin, M. J.; Zhang, A. P.; Qian, J. W.; He, S. L. *IEEE Sens. J.* **2012**, *12*, 1477.
(126) Dong, S. Y.; Luo, M.; Peng, G. D.; Cheng, W. H. *Sens. Actuators, B* **2008**, *129*, 94.
(127) Wu, S. Z.; Cheng, W. P.; Qiu, Y.; Li, Z. P.; Shuang, S. M.; Dong, C. A. *Sens. Actuators, B* **2010**, *144*, 255.
(128) Han, J.; Burgess, K. *Chem. Rev.* **2009**, *110*, 2709.
(129) Khan, M. A.; Alam, S. M.; Wabaidur, S. M.; Lee, S. H.; Suh, Y. S.; Choi, J. H. *Sens. Lett.* **2009**, *7*, 1.
(130) Jin, W. Z.; Wu, L. X.; Song, Y. L.; Jiang, J. J.; Zhu, X. D.; Yang, D. W.; Bai, C. X. *IEEE Trans. Biomed. Sci.* **2011**, *58*, 1232.
(131) Jokic, T.; Borisov, S. M.; Saf, R.; Nielsen, D. A.; Kühl, M.; Klimant, I. *Anal. Chem.* **2012**, *84*, 6723.
(132) Derinkuyu, S.; Ertekin, K.; Oter, O.; Denizalti, S.; Cetinkaya, E. *Dyes Pigm.* **2008**, *76*, 133.
(133) Wang, X.-D.; Meier, R. J.; Wolfbeis, O. S. *Adv. Funct. Mater.* **2012**, *22*, 4202.
(134) Borisov, S. M.; Herrod, D. L.; Klimant, I. *Sens. Actuators, B* **2009**, *139*, 52.
(135) Borisov, S. M.; Gatterer, K.; Klimant, I. *Analyst* **2010**, *135*, 1711.
(136) Goncalves, H. M. R.; Maule, C. D.; Jorge, P. A. S.; da Silva, J. *Anal. Chim. Acta* **2008**, *626*, 62.
(137) Saikia, R.; Buragohain, M.; Datta, P.; Nath, P.; Barua, K. *AIP Conf. Proc.* **2009**, *1147*, 249.
(138) Harvey, D.; Hayes, N. W.; Tighe, B. *Contact Lens Anterior Eye* **2012**, *35*, 137.
(139) Warren-Smith, S. C.; Heng, S.; Ebendorff-Heidepriem, H.; Abell, A. D.; Monro, T. M. *Langmuir* **2011**, *27*, 5680.
(140) Verma, N.; Kumar, S.; Kaur, H. *J. Biosens. Bioelectron.* **2010**, *1*, 102.
(141) Lin, T.-J.; Chung, M.-F. *Biosens. Bioelectron.* **2009**, *24*, 1213.
(142) Lin, T.-J.; Chung, M.-F. *Sensors* **2008**, *8*, 582.
(143) Liu, N.; Li, L. X.; Cao, G. H.; Lee, R. *J. Mater. Chem.* **2010**, *20*, 9029.
(144) Yin, M. J.; Gu, B. B.; Qian, J. W.; Zhang, A. P.; An, Q. F.; He, S. L. *Anal. Methods* **2012**, *4*, 1292.
(145) Long, F.; Gao, C.; Shi, H. C.; He, M.; Zhu, A. N.; Klibanov, A. M.; Gu, A. Z. *Biosens. Bioelectron.* **2011**, *26*, 4018.
(146) Yanaz, Z.; Filik, H.; Apak, R. *Sens. Actuators, B* **2010**, *147*, 15.
(147) Guillemain, H.; Rajarajan, M.; Sun, T.; Grattan, K. T. V. *Meas. Sci. Technol.* **2009**, *20*, 045207.
(148) Hayes, N. W.; Tremlett, C. J.; Melfi, P. J.; Sessler, J. D.; Shaw, A. M. *Analyst* **2008**, *133*, 616.
(149) Gu, B.; Yin, M.-J.; Zhang, A. P.; Qian, J.-W.; He, S. *Sens. Actuators, B* **2011**, *160*, 1174.
(150) Saleh, S. M.; Ali, R.; Wolfbeis, O. S. *Chem.—Eur. J.* **2011**, *17*, 14611.
(151) Gani, A. A.; Ashari, M. R.; Kuswandi, B. *Sens. Lett.* **2010**, *8*, 320.
(152) Balan Pillai, A.; Varghese, B.; Madhusoodanan, K. N. *Environ. Sci. Technol.* **2011**, *46*, 404.
(153) Nguyen, T. H.; Lin, Y. C.; Chen, C. T.; Surre, F.; Venugopalan, T.; Sun, T.; Grattan, K. T. V. *Proc. SPIE, Int. Soc. Opt. Eng.* **2009**, *7503*, 750314/1.
(154) Rahman, H. A.; Harun, S. W.; Yasin, M.; Phang, S. W.; Damanhuri, S. S. A.; Arof, H.; Ahmad, H. *Sens. Actuator A-Phys.* **2011**, *171*, 219.
(155) Possetti, G. R. C.; Kamikawachi, R. C.; Prevedello, C. L.; Muller, M.; Fabris, J. L. *Meas. Sci. Technol.* **2009**, *20*, 034003/1.
(156) Zhao, Y.; Zhang, X. Y.; Zhao, T. T.; Yuan, B.; Zhang, S. *IEEE Sens. J.* **2009**, *9*, 1148.
(157) Luzinova, Y.; Zdyrko, B.; Luzinov, I.; Mizaikoff, B. *Anal. Chem.* **2012**, *84*, 1274.
(158) Ma, J.; Kos, A.; Bock, W. J.; Li, X.; Nguyen, H.; Wang, Z. Y. *Proc. SPIE, Int. Soc. Opt. Eng.* **2011**, *7753*, 77535M/1.
(159) Nguyen, T. H.; Sun, T.; Grattan, K. T. V.; Hardwick, S. A. *Proc. SPIE, Int. Soc. Opt. Eng.* **2010**, *7653*, 76531V/1.
(160) Nguyen, T. H.; Hardwick, S. A.; Sun, T.; Grattan, K. T. V. *IEEE Sens. J.* **2012**, *12*, 255.
(161) Bansal, L.; El-Sherif, M. A. *Int. J. Smart Sensing Intell. Syst.* **2010**, *3*, 230.
(162) Jesus, C.; Silva, S. F. O.; Castanheira, M.; Gonzalez Aguilar, G.; Frazao, O.; Jorge, P. A. S.; Baptista, J. M. *Proc. SPIE, Int. Soc. Opt. Eng.* **2009**, *7503*, 75031A/1.
(163) Filik, H.; Aksu, D.; Apak, R.; Şener, İ.; Kılıç, E. *Sens. Actuators, B* **2009**, *136*, 105.
(164) Binu, S.; Pillai, V. R. M.; Pradeepkumar, V.; Padhy, B. B.; Joseph, C. S.; Chandrasekaran, N. *Mater. Sci. Eng., C* **2009**, *29*, 183.
(165) Tierney, S.; Volden, S.; Stokke, B. T. *Biosens. Bioelectron.* **2009**, *24*, 2034.
(166) Mader, H. S.; Wolfbeis, O. S. *Microchim. Acta* **2008**, *162*, 1.
(167) Libish, T. M.; Linesh, J.; Bobby, M. C.; Biswas, P.; Bandypadhyay, S.; Dasgupta, K.; Radhakrshnan, P. *Optoelectron. Adv. Mater.—Rapid Commun.* **2011**, *5*, 68.
(168) Fernandez-Novales, J.; Lopez, M. I.; Sanchez, M. T.; Garcia-Mesa, J. A.; Gonzalez-Caballero, V. *Int. J. Food Sci. Nutr.* **2009**, *60*, 265.
(169) Tewari, J. C.; Dixit, V.; Cho, B. K.; Malik, K. A. *Spectrochim. Acta, Part A* **2008**, *71*, 1119.
(170) Rosi, F.; Daveri, A.; Miliani, C.; Verri, G.; Benedetti, P.; Pique, F.; Brunetti, B. G.; Sgamellotti, A. *Anal. Bioanal. Chem.* **2009**, *395*, 2097.
(171) Han, C. L.; Min, A. X.; Chiu, C. C.; Shaillender, M.; Neu, B.; Wei Chang, W.; Peng, Z.; Kam Chew, L. *IEEE J. Sel. Top. Quantum Electron.* **2012**, *18*, 1457.
(172) Yue, J.; Zhang, L.; Yang, Z. *Int. J. Environ. Anal. Chem.* **2009**, *89*, 821.
(173) Leskinen, S. D.; Lim, D. V. *Appl. Environ. Microbiol.* **2008**, *74*, 4792.
(174) Chang, Y.-F.; Hung, S.-H.; Lee, Y.-J.; Chen, R.-C.; Su, L.-C.; Lai, C.-S.; Chou, C. *Anal. Chem.* **2011**, *83*, 5324.
(175) Chang, Y.-F.; Chen, R.-C.; Lee, Y.-J.; Chao, S.-C.; Su, L.-C.; Li, Y.-C.; Chou, C. *Biosens. Bioelectron.* **2009**, *24*, 1610.
(176) Huang, J. C.; Chang, Y.-F.; Chen, K.-H.; Su, L.-C.; Lee, C.-W.; Chen, C.-C.; Chen, Y.-M. A.; Chou, C. *Biosens. Bioelectron.* **2009**, *25*, 320.
(177) Chang, Y.-F.; Wang, S.-F.; Huang, J. C.; Su, L.-C.; Yao, L.; Li, Y.-C.; Wu, S.-C.; Chen, Y.-M. A.; Hsieh, J.-P.; Chou, C. *Biosens. Bioelectron.* **2010**, *26*, 1068.
(178) Rajarajan, M.; Dar, T.; Themistos, C.; Rahman, B. M. A.; Grattan, K. T. V.; Homola, J.; Irudayaraj, J. *J. Modern Opt.* **2009**, *56*, 564.
(179) Su, L.-C.; Chang, Y.-F.; Chou, C.; Ho, J.-a. A.; Li, Y.-C.; Chou, L.-D.; Lee, C.-C. *Anal. Chem.* **2011**, *83*, 3290.
(180) Chang, Y.-F.; Hsieh, J.-P.; Su, L.-C.; Li, Y.-C.; Lee, C.-C.; Chou, C. *Proc. SPIE, Int. Soc. Opt. Eng.* **2010**, *7759*, 77590H/1.
(181) Lin, C.-H.; Chen, H.-Y.; Yu, C.-J.; Lu, P.-L.; Hsieh, C.-H.; Hsieh, B.-Y.; Chang, Y.-F.; Chou, C. *Anal. Biochem.* **2009**, *385*, 224.
(182) Chang, Y.-F.; Chen, R.-C.; Li, Y.-C.; Yu, C.-J.; Hsieh, B.-Y.; Chou, C. *Proc. SPIE, Int. Soc. Opt. Eng.* **2007**, *6826*, 68261B/1.
(183) Kapoor, R.; Wang, C.-W. *Biosens. Bioelectron.* **2009**, *24*, 2696.
(184) Wang, C. W.; Manne, U.; Reddy, V. B.; Oelschlager, D. K.; Katkoori, V. R.; Grizzle, W. E.; Kapoor, R. *J. Biomed. Opt.* **2010**, *15*, 067005.
(185) Wang, C.-W.; Manne, U.; Reddy, V. B.; Kapoor, R. *Proc. SPIE, Int. Soc. Opt. Eng.* **2010**, *7559*, 75590G.
(186) Zhang, Y.; Zeng, Q.; Sun, Y.; Liu, X.; Tu, L.; Kong, X.; Buma, W. J.; Zhang, H. *Biosens. Bioelectron.* **2010**, *26*, 149.
(187) Leung, A.; Shankar, P. M.; Mutharasan, R. *Sens. Actuators, B* **2008**, *129*, 716.
(188) Ohk, S. H.; Koo, O. K.; Sen, T.; Yamamoto, C. M.; Bhunia, A. K. *J. Appl. Microbiol.* **2010**, *109*, 808.
(189) Valadez, A.; Lana, C.; Tu, S.-I.; Morgan, M.; Bhunia, A. *Sensors* **2009**, *9*, 5810.
(190) Long, F.; Wu, S.; He, M.; Tong, T.; Shi, H. *Biosens. Bioelectron.* **2011**, *26*, 2390.

(191) Leung, A.; Shankar, P. M.; Mutharasan, R. *Sens. Actuators, B* **2008**, *131*, 640.
(192) Knez, K.; Janssen, K. P. F.; Pollet, J.; Spasic, D.; Lammertyn, J. *Small* **2012**, *8*, 868.
(193) Filip, D.; Jeroen, P.; Kris, J.; Bert, V.; Karel, K.; Dragana, S.; Jeroen, L. *Nanotechnology* **2012**, *23*, 065503.
(194) Ehrentreich-Förster, E.; Orgel, D.; Krause-Griep, A.; Cech, B.; Erdmann, V.; Bier, F.; Scheller, F.; Rimmele, M. *Anal. Bioanal. Chem.* **2008**, *391*, 1793.
(195) Saxl, T.; Khan, F.; Ferla, M.; Birch, D.; Pickup, J. *Analyst* **2011**, *136*, 968.
(196) Weidemaier, K.; Lastovich, A.; Keith, S.; Pitner, J. B.; Sistare, M.; Jacobson, R.; Kurisko, D. *Biosens. Bioelectron.* **2011**, *26*, 4117.
(197) Liao, K. C.; Hogen-Esch, T.; Richmond, F. J.; Marcu, L.; Clifton, W.; Loeb, G. E. *Biosens. Bioelectron.* **2008**, *23*, 1458.
(198) Saleh, S.; Ali, R.; Hirsch, T.; Wolfbeis, O. S. *J. Nanopart. Res.* **2011**, *13*, 4603.
(199) Bhatia, P.; Gupta, B. D. *Sens. Actuators, B* **2012**, *161*, 434.
(200) Schrenkhammer, P.; Wolfbeis, O. S. *Biosens. Bioelectron.* **2008**, *24*, 994.
(201) Zhong, Z.; Fritzsche, M.; Pieper, S. B.; Wood, T. K.; Lear, K. L.; Dandy, D. S.; Reardon, K. F. *Biosens. Bioelectron.* **2011**, *26*, 2407.
(202) Huang, J.; Fang, H.; Liu, C.; Gu, E.; Jiang, D. *Anal. Lett.* **2008**, *41*, 1430.
(203) Bidmanova, S.; Chaloupkova, R.; Damborsky, J.; Prokop, Z. *Anal. Bioanal. Chem.* **2010**, *398*, 1891.
(204) Das, N.; Reardon, K. F. *Anal. Lett.* **2012**, *45*, 251.
(205) Kudo, H.; Sawai, M.; Wang, X.; Gessei, T.; Koshida, T.; Miyajima, K.; Saito, H.; Mitsubayashi, K. *Sens. Actuators, B* **2009**, *141*, 20.
(206) Kudo, H.; Sawai, M.; Suzuki, Y.; Wang, X.; Gessei, T.; Takahashi, D.; Arakawa, T.; Mitsubayashi, K. *Sens. Actuators, B* **2010**, *147*, 676.
(207) Kudo, H.; Suzuki, Y.; Gessei, T.; Takahashi, D.; Arakawa, T.; Mitsubayashi, K. *Biosens. Bioelectron.* **2010**, *26*, 854.
(208) Kudo, H.; Wang, X.; Suzuki, Y.; Ye, M.; Yamashita, T.; Gessei, T.; Miyajima, K.; Arakawa, T.; Mitsubayashi, K. *Sens. Actuators, B* **2012**, *161*, 486.
(209) Eltzov, E.; Pavluchkov, V.; Burstin, M.; Marks, R. S. *Sens. Actuators, B* **2011**, *155*, 859.
(210) Eltzov, E.; Marks, R. S.; Voost, S.; Wullings, B. A.; Heringa, M. B. *Sens. Actuators, B* **2009**, *142*, 11.
(211) Eltzov, E.; Marks, R. S. In *Whole Cell Sensing Systems I: Reporter Cells and Devices*, Vol. *117*; Belkin, S., Gu, M. B., Eds.; Springer−Verlag: Berlin, Heidelberg, 2010; p 131.
(212) Verma, N.; Bansal, M.; Kumar, S. *Adv. Appl. Sci. Res.* **2012**, *3*, 809.
(213) Pena-Vazquez, E.; Maneiro, E.; Perez-Conde, C.; Moreno-Bondi, M. C.; Costas, E. *Biosens. Bioelectron.* **2009**, *24*, 3538.
(214) Ciprian, D.; Hlubina, P. *Proc. SPIE, Int. Soc. Opt. Eng.* **2012**, *8439*, 843927.
(215) Singh, S.; Gupta, B. D. *Meas. Sci. Technol.* **2010**, *21*, 115202.
(216) Zhang, Q.; Xue, C.; Yuan, Y.; Lee, J.; Sun, D.; Xiong, J. *Sensors* **2012**, *12*, 2729.
(217) Lin, H.-Y.; Huang, C.-H.; Liu, Y.-C.; Huang, K.-W.; Chau, L.-K. *Proc. SPIE, Int. Soc. Opt. Eng.* **2012**, *8351*, 83512S.
(218) Han, M.; Wang, Y.; Wang, Y.; Wang, A. *Opt. Lett.* **2009**, *34*, 100.
(219) Yue, W.; Zhou, A.; He, B.; Cai, X. *Sens. Actuators, B* **2008**, *130*, 21.
(220) Wang, X.-D.; Meier, R. J.; Link, M.; Wolfbeis, O. S. *Angew. Chem., Int. Ed.* **2010**, *49*, 4907.
(221) Meier, R. J.; Schreml, S.; Wang, X.-D.; Landthaler, M.; Babilas, P.; Wolfbeis, O. S. *Angew. Chem., Int. Ed.* **2011**, *50*, 10893.
(222) Xiong, F. B.; Djeu, N.; Zhu, W. Z. *Sens. Lett.* **2012**, *10*, 60.
(223) Phang, S.; Yang, H.; Harun, S.; Arof, H.; Ahmad, H. *J. Optoelectron. Adv. Mater.* **2011**, *13*, 604.
(224) Bharadwaj, R.; Sai, V. V. R.; Thakare, K.; Dhawangale, A.; Kundu, T.; Titus, S.; Verma, P. K.; Mukherji, S. *Biosens. Bioelectron.* **2011**, *26*, 3367.
(225) Gomez, A. L.; Renzi, R. F.; Fruetel, J. A.; Bambha, R. P. *Appl. Opt.* **2012**, *51*, 2532.
(226) Renganathan, B.; Sastikumar, D.; Gobi, G.; Srinivasan, R.; Rajeshwari Yogamalar, N.; Chandra Bose, A. *Proc. SPIE, Int. Soc. Opt. Eng.* **2010**, *7764*, 77640U.
(227) Chatni, M. R.; Maier, D. E.; Porterfield, D. M. *Sens. Actuators, B* **2009**, *141*, 471.
(228) Ng, M.-Y.; Liu, W.-C. *Opt. Express* **2009**, *17*, 5867.
(229) Funfak, A.; Cao, J.; Wolfbeis, O.; Martin, K.; Köhler, J. *Microchim. Acta* **2009**, *164*, 279.
(230) Stich, M. I. J.; Nagl, S.; Wolfbeis, O. S.; Henne, U.; Schaeferling, M. *Adv. Funct. Mater.* **2008**, *18*, 1399.
(231) Yu, X.; Zhang, Y.; Kwok, Y. C.; Shum, P. *Sens. Actuators, B* **2010**, *145*, 110.
(232) Woliński, T. R.; Tefelska, M. M.; Chychłowski, M. S.; Godyń, K.; Dąbrowski, R.; Wójcik, J.; Nasiłowski, T.; Thienpont, H. *Mol. Cryst. Liq. Cryst.* **2009**, *502*, 220.
(233) Xu, X.; Goponenko, A. V.; Asher, S. A. *J. Am. Chem. Soc.* **2008**, *130*, 3113.
(234) Shin, J.; Braun, P. V.; Lee, W. *Sens. Actuators, B* **2010**, *150*, 183.
(235) Xuan, R.; Wu, Q.; Yin, Y.; Ge, J. *J. Mater. Chem.* **2011**, *21*, 3672.
(236) Tian, E.; Wang, J.; Zheng, Y.; Song, Y.; Jiang, L.; Zhu, D. *J. Mater. Chem.* **2008**, *18*, 1116.
(237) Ge, J.; Yin, Y. *Angew. Chem., Int. Ed.* **2011**, *50*, 1492.
(238) Euser, T. G.; Chen, J. S. Y.; Scharrer, M.; Russell, P. S. J.; Farrer, N. J.; Sadler, P. J. *J. Appl. Phys.* **2008**, *103*, 103108/1.